ANTIOXIDANTS & REDOX SIGNALING
Volume 36, Numbers 4–6, 2022

DOI: 10.1089/ars.2021.0195

Discoveries

FORUM REVIEW ARTICLE

Chemiluminescence Measurement of Reactive Sulfur and Nitrogen Species

Bo Li,[1] Yujin Lisa Kim,[1] and Alexander Ryan Lippert[1,2,i]

Abstract

Significance: Reactive sulfur and nitrogen species such as hydrogen sulfide (H_2S) and nitric oxide ($NO^{\bullet}$) are ubiquitous cellular signaling molecules that play central roles in physiology and pathophysiology. A deeper understanding of these signaling pathways will offer new opportunities for therapeutic treatments and disease management.
Recent Advances: Chemiluminescence methods have been fundamental in detecting and measuring biological reactive sulfur and nitrogen species, and new approaches are emerging for imaging these analytes in living intact specimens. Ozone-based and luminol-based chemiluminescence methods have been optimized for quantitative analysis of hydrogen sulfide and nitric oxide in biological samples and tissue homogenates, and caged luciferin and 1,2-dioxetanes are emerging as a versatile approach for monitoring and imaging reactive sulfur and nitrogen species in living cells and animal models.
Critical Issues: This review article will cover the major chemiluminescence approaches for detecting, measuring, and imaging reactive sulfur and nitrogen species in biological systems, including a brief history of the development of the most established approaches and highlights of the opportunities provided by emerging approaches.
Future Directions: Emerging chemiluminescence approaches offer new opportunities for monitoring and imaging reactive sulfur and nitrogen species in living cells, animals, and human clinical samples. Widespread adoption and translation of these approaches, however, requires an emphasis on rigorous quantitative methods, reproducibility, and effective technology transfer. *Antioxid. Redox Signal*. 36, 337–353.

Keywords: chemiluminescence, reactive sulfur species, reactive nitrogen species

Introduction

Reactive sulfur and nitrogen species are small cellularly produced molecules that mediate signaling in healthy physiology (2, 39, 56). However, they can contribute to pathophysiological conditions when levels are too low or too high and thus precise measurement of these species is required to attain a complete understanding of their biological roles. Nitric oxide ($NO^{\bullet}$) was thrust into prominence in the 1980s when it was discovered that it could activate guanylyl cyclase and serve as an endothelium-derived relaxation factor to relax smooth muscle cells—discoveries that would eventually be rewarded with a Nobel prize in 1998 (63).

Nitric oxide is enzymatically produced by three isoforms of the nitric oxide synthase (NOS) enzyme—neuronal NOS (nNOS, NOS-1), inducible NOS (iNOS, NOS-2), and endothelial NOS (eNOS, NOS-3), each of which uses L-arginine as a precursor and requires heme, tetrahydrobiopterin (BH4), flavin adenine dinucleotide (FAD), and flavin mononucleotide (FMN) cofactors (120). Nitric oxide can also be produced by bacterial nitrate reduction in the microbiome followed by nitrite reduction (19). This small, diffusible, and reactive molecule plays important and central physiological and pathophysiological roles in the cardiovascular system (37), brain (46), cancer (12), gastrointestinal tract (133), lungs (7), and even in psychological stress (105).

[1]Department of Chemistry, Southern Methodist University, Dallas, Texas USA.
[2]Center for Drug Discovery, Design, and Delivery (CD), Southern Methodist University, Dallas, Texas USA.
[i]ORCID ID (https://orcid.org/0000-0003-4396-0848).

Canonical nitric oxide signaling begins with nitric oxide binding to guanylyl cyclase, increasing the rate of conversion of guanosine triphosphate (GTP) into cyclic guanosine monophosphate (cGMP), which, in turn, can modulate signaling *via* cGMP-dependent protein kinases (PKGs), cGMP-gated cation channels, phosphodiesterases (PDEs), and other targets (40). In addition, nitric oxide is a reactive molecule that gives rise to a host of reactive nitrogen species (56) that can also participate in cellular signaling (2), including (but not limited to) *S*-nitroso proteins and small molecules (34), peroxynitrite ($ONOO^-$) and decomposition products (38), nitroxyl (HNO) (41, 64), and nitrite/nitrate (31). Taken together, these progenies of nitric oxide are collectively referred to as reactive nitrogen species.

Hydrogen sulfide (H_2S) is another small, reactive, and diffusible molecule that is enzymatically produced in mammalian systems by cystathionine γ-lyase (CSE), cystathionine β-synthase (CBS), and 3-mercaptopyruvate sulfur transferase (3-MST) (65). Endogenous levels of hydrogen sulfide are controlled, in part, by catabolic enzymes sulfide:quinone reductase (SQR) and persulfide dioxygenase, ETHE1. Hydrogen sulfide can also be produced by the microbiome *via* reduction of dietary sulfates to play important roles in mammalian biology (19). Hydrogen sulfide can mediate cellular signaling in a number of physiological scenarios by means of persulfide and polysulfide (H_2S_n) formation, binding to metal centers, and interaction with other reactive sulfur, oxygen (O_2), and nitrogen species (39).

Similar to nitric oxide, hydrogen sulfide has emerged as a ubiquitous mediator of physiology in a number of tissues and organs (39). Hydrogen sulfide is present in aortic tissue at levels that are $20-100$ times higher than other tissues (77), and the actions of hydrogen sulfide have been well studied in the cardiovascular system (19, 101, 142). It has also been studied in the brain and gut, where some of the first evidence for hydrogen sulfide's signaling roles was observed (1, 71).

A related class of reactive sulfur species central to hydrogen sulfide signaling comprises polysulfide/sulfane sulfurs that contain sulfur in the S^0 oxidation state with a sulfur–sulfur bond (86). Polysulfides can be formed by oxidation of hydrogen sulfide (24), but enzymatic synthesis by the same enzymes that form hydrogen sulfide, CBS, CSE (62), and 3-MST (97) are more likely to be physiologically relevant avenues of polysulfide formation *via* generation of cysteine persulfide (Cys-SSH).

Quite interestingly, cysteinyl-tRNA synthetases (CARSs) were found to be able to mediate persulfidation to form Cys-SSH, in addition to incorporating Cys-SSH into proteins, accounting for a large percentage of protein persulfidation (3). Other potential avenues for persulfide generation include heme proteins such as superoxide dismutase (SOD) (99) and myeloperoxidase (MPO) (44). The catabolism of polysulfides is less understood, but it has been shown that thioredoxin and glutathione systems can mediate this conversion (33). A number of proteins have been shown to be targets of persulfidation, including NF-E2 p45-related factor (Nrf2), Kelch-like ECH-associated protein (Keap1), heme oxygenase-1 (HO-1), phosphatase and tensin homolog (PTEN), and protein kinase G-1α (PKG1α) (86).

Indeed, there is an emerging realization that polysulfide signaling is a central component of reactive sulfur signaling in cardiovascular disease and other biological systems (73). It should be emphasized that polysulfide chemistry is quite complex (75), and that reactive sulfur and nitrogen species interact both chemically (39) and biologically (19). When combined with reactive oxygen and carbon species, they form a complex web of interacting species that has been referred to as the reactive species interactome (28).

Given the importance of reactive sulfur and nitrogen species in physiology and pathophysiology, their measurement and detection in biological systems is of the utmost importance to increase fundamental understanding and develop therapeutic approaches. Due to their reactive nature, one class of methods that is particularly well suited for measuring reactive sulfur and nitrogen species is chemiluminescence.

Chemiluminescence is the light generated from a thermal reaction that leads to the production of a molecule in an emissive excited state (128). Most (although not all) chemiluminescent reactions involve the cleavage of a weak oxygen–oxygen bond in a structure with a large ring strain, leading to a highly exothermic reaction. The key advantage of chemiluminescence is that the background signal is quite low due to the elimination of an external light source; this ultimately leads to a large increase in sensitivity and offers opportunities for deep tissue imaging (109).

This review article will focus on chemiluminescence methods for the detection of reactive sulfur and nitrogen species, which have been a critical tool in developing an understanding of hydrogen sulfide and nitric oxide in biological systems. We note that chemiluminescence methods for measuring reactive oxygen species have been recently reviewed (122). The structure of this review will be roughly chronological, starting with well-established and commercialized ozone (O_3)-based and luminol chemiluminescence techniques and ending with emerging luciferin/luciferase, 1,2-dioxetane, and nanotechnology strategies.

Ozone-Based Chemiluminescence

Ozone-based chemiluminescence detection of hydrogen sulfide

Gas chromatography with ozone-induced sulfur chemiluminescence has become a powerful method of choice for measuring biological hydrogen sulfide (131) and is the result of extensive fundamental and applied research (139–141). The spectrum of the sulfur ''afterglow'' of sulfur dioxide (SO_2) was first reported in 1934 (47), and the chemiluminescent reaction of sulfur monoxide (SO) with ozone to produce SO_2 in the excited state was reported in 1966 (Fig. 1A, Equations 1 and 2) (54).

It was later shown that a range of sulfur-containing molecules, including SO, hydrogen sulfide, and other sulfur species, can undergo combustion and be reacted with ozone to form a species with a spectrum that is identical to that of SO_2 (4, 74). This chemiluminescence emission spectrum has a maximum at ~ 350 nm and extends from 280 to 450 nm (4, 54, 74, 131). These identical spectra lead to the conclusion that the reaction of ozone with sulfur species ultimately produces the same emitting species, excited state SO_2. SO has been proposed as a common intermediate, and studies on the reaction of methyl mercaptan with hydrogen sulfide further support a mechanism with hydrosulfinyl radical ($HSO^\bullet$) and SO as important intermediates (Fig. 1A, Equations 3–5) (50).

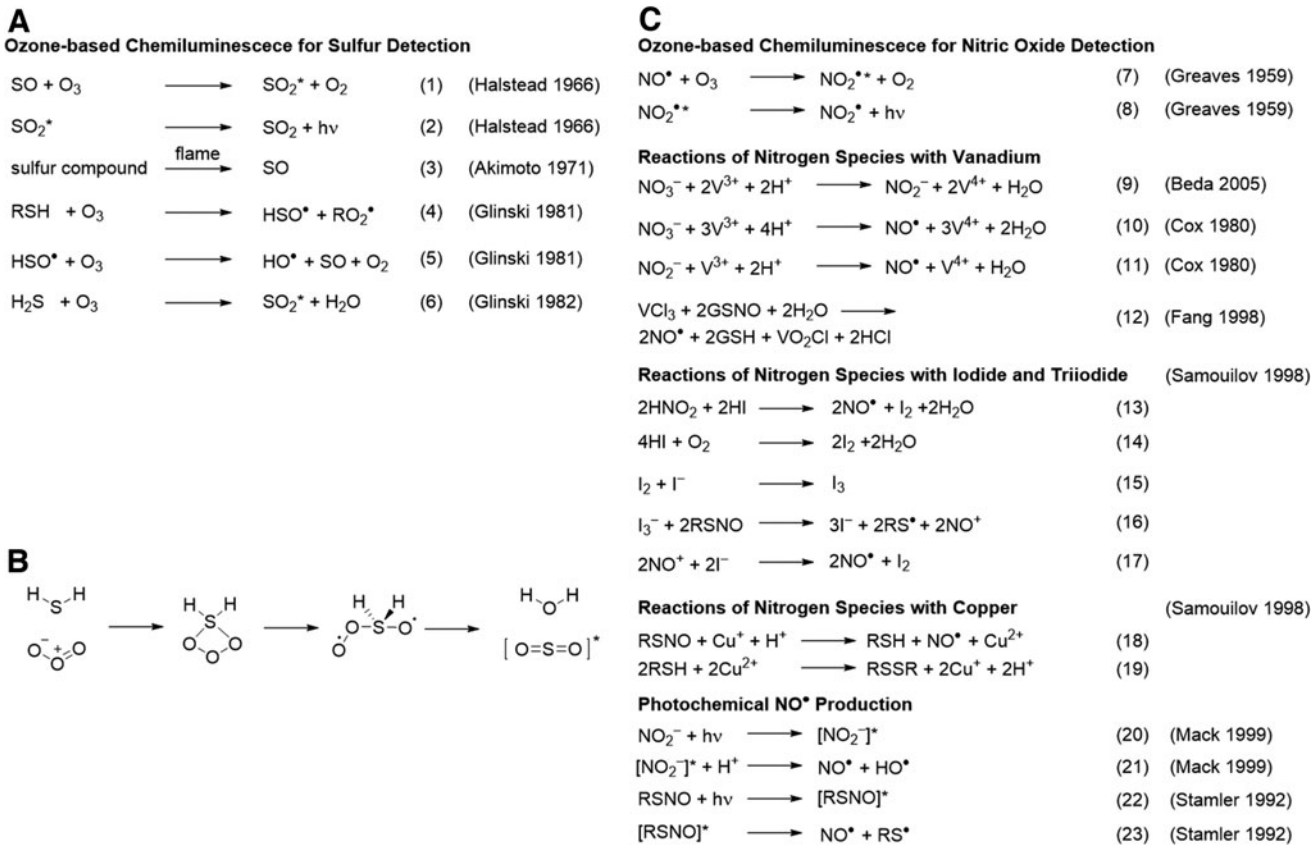

FIG. 1. Reactions involved in ozone-based chemiluminescence. (A) Reactions for ozone-based chemiluminescence detection of sulfur species. **(B)** Mechanism for the reaction of hydrogen sulfide and ozone. **(C)** Reactions for ozone-based chemiluminescence detection of nitrogen species.

Interestingly, experiments done at a low pressure to ensure single collisions showed that H_2S can react directly with ozone to produce chemiluminescence (Fig. 1A, Equation 6) with the proposed mechanism as shown in Figure 1B proceeding through a strained 4-membered ring intermediate with two oxygen–oxygen bonds (49). Further, red-shifted chemiluminescence emission that extends to the near-infrared (NIR) spectrum has been observed for the reaction of hydrogen sulfide and ozone and attributed to emission from the excited radical species $HSO^{\bullet}$ (115).

It was not long after these chemiluminescent reactions were understood that efforts turned toward harnessing them as an analytical technique for measuring sulfur compounds. It was first shown that a chemiluminescent aerosol spray consisting of O_3/O_2 mixtures could be used in conjunction with liquid chromatography for the detection of sulfur compounds (15). Later, researchers developed a Universal Sulfur Detection strategy by exposing sulfur-containing compounds, including hydrogen sulfide, to a hydrogen flame followed by a reaction with ozone to produce chemiluminescence *via* an SO intermediate (13). This detector was combined with gas chromatography separation and improved to form the basis of commercial gas chromatography/sulfur chemiluminescence systems (116, 117).

We also note that sulfur compounds can be reacted with fluorine gas to generate chemiluminescence and chromatographic systems with fluorine-based chemiluminescence detection have been developed (94). Safety issues with working with toxic fluorine gas, however, have likely made commercialization of these systems less viable.

On the development and commercialization of gas chromatography with sulfur chemiluminescence detection, methods and techniques were optimized for studying biological hydrogen sulfide. Early adoption of this technology for biological systems used it to study hydrogen sulfide production and metabolism in the digestive system (43, 78, 123).

This chemiluminescent technique was then used to revise reported estimates of micromolar tissue levels of free hydrogen sulfide to the now more widely accepted nanomolar levels (42). This study measured hydrogen sulfide in the headspace of tissue homogenates and in exhaled breath and was validated by recovery of 2.7 μM sulfide added to a buffer. In a convincing demonstration, an injection of 50 μM sulfide into brain homogenates (the putative estimate of biological sulfide levels at the time) completely swamped any signal from endogenous sulfide. The same group followed up on this discrepancy by showing that ''acid-labile'' sulfur pools were released at micromolar levels and explained the differing values that were measured (77). Interestingly, high levels of free hydrogen sulfide ($\sim 1\ \mu M$) were observed in aortic tissues, suggesting important roles for hydrogen sulfide in cardiovascular function.

Gas chromatography with sulfur chemiluminescence was also used to identify contributions from CBS and CSE enzymes that were responsible for hydrogen sulfide production (66). This study examined mouse tissues, including liver, kidney, and brain, and showed both enhancement using *S*-adenosylmethionine, an allosteric regulator of CBS, and attenuation using propargyl glycine, an irreversible inhibitor of CSE. Further, this chemiluminescence method was used to provide quantitative measures of the kinetics of hydrogen sulfide production and metabolism in liver, brain, and kidney homogenates and provided steady-state estimates of tissue hydrogen sulfide in the nanomolar range (132). Polysulfides/sulfane sulfur can also be measured with this technique by first releasing hydrogen sulfide from sulfane sulfur by treatment with dithiothreitol (DTT) (72).

Ozone-based chemiluminescence is now a standard technique for measuring hydrogen sulfide in tissue homogenates and has become a method of choice in recent studies from several research groups (137, 138). We direct the reader to the work by Vitvitsky and Banerjee for procedures on using ozone chemiluminescence to measure biological hydrogen sulfide (131).

Ozone-based chemiluminescence detection of nitric oxide

Red to NIR chemiluminescence emission from the reaction of nitric oxide and ozone was first studied in 1959 (Fig. 1C, Equations 7 and 8), where an observed emission that spanned a wavelength range from 590 to 1085 nm was attributed to the excited state of nitrogen dioxide radical ($NO_2^\bullet$) based on spectral and thermodynamic analyses (52). Detailed kinetic (27) and mechanistic (26) studies confirmed a bimolecular reaction and second-order rate equation between nitric oxide and ozone to produce the emissive nitrogen dioxide species, with the overall emission intensity being proportional to the concentration of nitric oxide. In addition, a corrected spectrum with measurements up to 3200 nm showed that the peak emission was centered at 1200 nm and extended from 590 nm up to 2400 nm (26).

It is important to note that the wide spectral separation between the emission of SO_2 and $NO_2^\bullet$ enables selectivity between sulfur and nitrogen detection by using ozone-based chemiluminescence (139). An understanding of this chemiluminescence reaction led to its application as an analytical technique (8), initially for studying atmospheric, dissolved, and photolytically released nitric oxide in sea water (143). Soon after, its use for detecting biological nitric oxide proved to be transformative and was one of the methods used to confirm nitric oxide as the endothelium-derived relaxation factor (100).

This method was further optimized for direct detection of nitric oxide in biological and clinically relevant scenarios, including nitric oxide release from nitrovasodilator drugs (17, 93). Although ozone-based chemiluminescence is used for the direct detection of nitric oxide, the short lifetime of nitric oxide in the presence of oxygen, metals, and other biomolecules is an obstacle because sampling or homogenizing tissues often takes longer than the lifetime of nitric oxide under these conditions. For this reason, emphasis has been placed on tracking more stable end products of nitric oxide such as nitrite, *S*-nitroso compounds, and *N*-nitroso compounds that can be re-converted to nitric oxide by using reductive (11, 58, 88) and photolytic methods (92, 119).

Early methods for environmental nitrite analysis used vanadium(III) (16) (Fig. 1C, Equations 9 – 11) or iodide (29, 45) (Fig. 1C, Equations 13 – 17) to reduce nitrite and nitrate to nitric oxide before detection with ozone-based chemiluminescence. Vanadium chloride can be used to reduce both nitrate (Fig. 1C, Equations 9 and 10) and nitrite (Fig. 1C, Equation 11) (16, 20, 29). It soon became appreciated that vanadium (36) and iodide (110) could also release nitric oxide from *S*-nitroso groups (Fig. 1C, Equations 12 and 16).

Photolytic methods were developed to homolytically cleave the S – N bond of *S*-nitroso thiols (Fig. 1C, Equation 22 and 23) (119). These methods were used to show that vanadium reactions could misidentify *S*-nitroso compounds as nitrate, and a copper-based assay for *S*-nitroso compounds was developed to solve this problem (Fig. 1C, Equations 18 and 19) (36). Although some vanadium-mediated release of nitric oxide from *S*-nitroso compounds is, indeed, observed, a more complete measurement of *S*-nitroso compounds was accomplished by first releasing nitrite from the S – N bond using mercury (35), *via* the Saville reaction (111), followed by ozone-based chemiluminescence detection.

For accurate *S*-nitroso compound measurements, interferences from nitrite can be mitigated by first reacting nitrites in the sample with sulfanilimide in a diazotization reaction, and interferences from nitrosation of free thiols can be mitigated by pretreatment with *N*-ethylmaleimide to cap any free thiols and prevent reactions that recapture released nitric oxide (88, 91). Carbon monoxide can be added to prevent recapture of nitric oxide by iron–heme complexes (11, 32). Iodide and hydroxyquinone were also shown to generate nitric oxide for ozone-based chemiluminescence, with hydroxyquinone being more selective for *S*-nitroso compounds (110).

Similar ozone-based chemiluminescence methods have been developed to measure nitrosylhemoglobin [Hb(II)NO] (96) and dintrosyl iron complexes (95). Photolytic methods to cleave the S – N bond are complicated by known photochemistry of nitrite (Fig. 1C, Equations 20 and 21) (89), whereas reductive methods are complicated by nitric oxide release from diverse nitrogen-containing species, including nitrate, nitrite, *S*-nitroso compounds, and *N*-nitroso compounds.

Although the precise interpretations and methods for quantifying nitric oxide, nitrite, and *S*-nitroso compounds has been the subject of healthy debate, direct comparisons of different methods suggest that all can provide useful information when interpreted correctly and the use of more than one method improves confidence in results (11). The interested reader is directed to the work of Basu *et al.* for procedures (11).

Luminol and L-012 Chemiluminescence Detection of Reactive Sulfur and Nitrogen Species

Luminol and derivatives such as 8-amino-5-chloro-2,3-dihydro-7-phenyl-pyrido[3,4-d]pyridazine-1,4-dione (L-012) (98) have been used for the sensitive detection of peroxynitrite (102), nitrogen dioxide (90), nitric oxide (70), and other oxidative species. Luminol can directly react with $NO_2^\bullet$ without the need for a catalyst, and this reaction was used to develop an instrument to measure $NO_2^\bullet$ and peroxy radicals in the atmosphere (Fig. 2A) (21, 24, 68, 90, 135). Luminol can also be used for peroxynitrite detection in a process that is enhanced by the addition of carbonate and inhibited by SOD (Fig. 2B) (103).

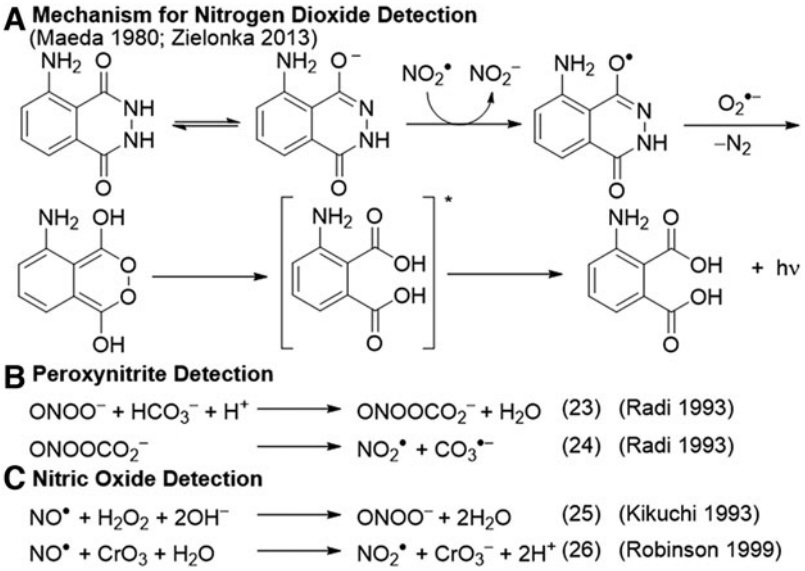

FIG. 2. Reactions for the chemiluminescence detection of reactive nitrogen species with luminol.

The originally proposed mechanism involves the adduct of peroxynitrite and carbon dioxide mediating a one-electron oxidation of luminol, with the formation of superoxide that reacts with the luminol radical to yield the light-emitting endoperoxide. Studies of the luminol derivative L-012 revealed that it likely reacts with radical species derived from peroxynitrite such as carbonate radical or nitrogen dioxide radical, as evidenced by an increase in signal with the addition of carbonate (30). Further, it was shown that superoxide can actually be formed in the course of the peroxynitrite oxidation of L-012, making it possible to form the endoperoxide in the absence of any additional superoxide (149). The complexity of these reactions demands careful evaluation of mechanistic considerations when using luminol and derivatives for analytical assays.

Luminol has been used to detect nitric oxide in a luminol-H_2O_2 (hydrogen peroxide) system, through the reaction of $NO^{\bullet}$ and H_2O_2 to form peroxynitrite (Fig. 2C) (70). The authors provided ultraviolet/visible evidence of peroxynitrite production, showed that the assay is independent of superoxide inhibition by SOD, and neither $NO_2^{\bullet}$ nor hydroxyl radical ($HO^{\bullet}$) was detected. The assay was used in a flow organ perfusion system to measure $NO^{\bullet}$ in the kidneys. A later study was unable to detect $NO^{\bullet}$ by using the same luminol-H_2O_2 system but it did observe that the oxidation of $NO^{\bullet}$ to $NO_2^{\bullet}$ with chromium trioxide (CrO_3) before exposure to luminol-H_2O_2 greatly enhanced the signal. This chemistry was used to develop an instrument for measuring $NO^{\bullet}$ in the exhaled breath (Fig. 2C) (106).

The luminol derivative L-012 was shown to be capable of detecting peroxynitrite and gave a signal $\sim$100-fold higher than that of luminol (Fig. 3A) (30). The system showed a response from synthetic $ONOO^-$, the peroxynitrite donor 3-morpholinosydnonimine (SIN-1), and a continuous enzymatic superoxide production system [hypoxanthine/xanthine oxidase and diethylammonium (Z)-1-(N,N-diethylamino) diazen-1-ium-1,2-diolate (DEA NONOate)]. The response was validated and compared with other chemiluminescence assays and high-performance liquid chromatography (HPLC) analysis of dihydroethidium. Controls using the $NO^{\bullet}$ scavenger 2-phenyl-4,4,5,5-tetramethylimidazoline-1-oxy 3-oxide (PTIO), the superoxide scavenger SOD, and an iNOS inhibitor provided a selective assay and it was demonstrated that L-012 could detect peroxynitrite formed from superoxide generated in isolated mitochondria.

Interestingly, L-012 has also been used for *in vivo* imaging of inflammation (69), where it showed significant increases in luminescent signal *versus* controls in mice injected with L-012 and various inflammatory stimulators including lipopolysaccharide (LPS), phorbol 12-myristate 13-acetate (PMA), and in an arthritis inflammation model. A strong signal was observed in the intestine, even under baseline conditions, and a weaker signal was seen in the lungs and spleen. Strong inhibition by the nitric oxide inhibitor N (ω)-nitro-L-arginine methyl ester (L-NAME) suggests that peroxynitrite is responsible for the observed signal.

A luminol-based system has been used for the detection of hydrogen sulfide by masking the aniline nitrogen of luminol with an azide group that can be reduced by H_2S (Fig. 3B, C) (9, 10). The masked luminol derivative is first incubated with a sample containing hydrogen sulfide, which reduces the azide to an amine to form the free luminol derivative. The sample is then mixed with horseradish peroxidase, H_2O_2, and *para*-iodophenol to oxidize the luminol derivative and generate chemiluminescence. The *para*-iodophenol is a chemiluminescence enhancer that increases the rate of formation of luminol radicals. It was observed that the isoluminol derivative with the azide at the meta position, named **CLSS-2**, displayed better selectivity for H_2S over other thiol species and was used to measure enzymatically generated H_2S.

Luminol systems offer high sensitivity for reactive species and can provide useful information when combined with the appropriate controls. This caged luminol strategy is an innovative approach that provides ample opportunity for further exploration.

Bioluminescent Caged Luciferin Probes for Reactive Sulfur and Nitrogen Species

A ''caged'' luciferin is a luciferin derivative that is not a luminescent substrate for a bioluminescent enzyme but, after reaction with a targeted analyte or set of conditions, is

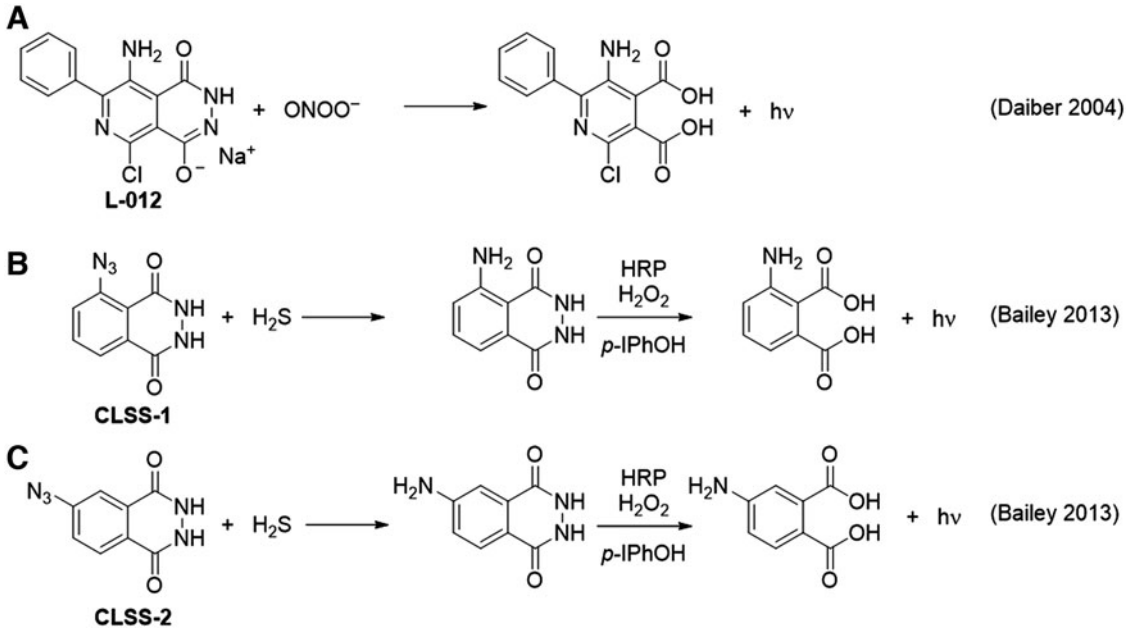

FIG. 3. Reactions of luminol derivatives for the detection of reactive nitrogen and sulfur species.

''uncaged'' and converted into a substrate that can generate bioluminescence. Luciferase catalyzes the chemiluminescent reaction of luciferin by using adenosine triphosphate, magnesium, and oxygen *via* an intermediate dioxetanone structure (Fig. 4). Caged luciferins offer a chemiluminescent signal that can be combined with genetically modified models for cellular studies and *in vivo* imaging (121). Given the versatility of this method, many examples of using caged and modified luciferins for reactive sulfur, oxygen, and nitrogen species have been reported (Figs. 5–7) (144).

Originally demonstrated to be a bioluminescence probe for H_2O_2 (129, 130), the boronate-based probe **PCL-1** also reacts with $ONOO^-$ and hypochlorite (HOCl) to convert the boronate to a phenol, followed by a spontaneous self-immolative cleavage to release luciferin (Fig. 5) (118). It was observed that catalase inhibited **PCL-1** signal from LPS-treated macrophages, whereas the iNOS inhibitor L-NAME alone did not, suggesting that at least some of the observed signal is from H_2O_2. The strongest inhibition was seen from a combination of catalase and L-NAME, suggesting that both peroxynitrite and H_2O_2 generated signals in this system.

Detailed studies of the reaction products with H_2O_2, HOCl, and $ONOO^-$ show clean conversion to luciferin with H_2O_2, formation of luciferin and a chlorinated product with HOCl, and formation of luciferin and a nitrated product with $ONOO^-$ (150). This study further shows that combining bioluminescence imaging with HPLC analysis of product distributions coupled with proper controls can be used for more rigorous identification of which species are generated during an experiment.

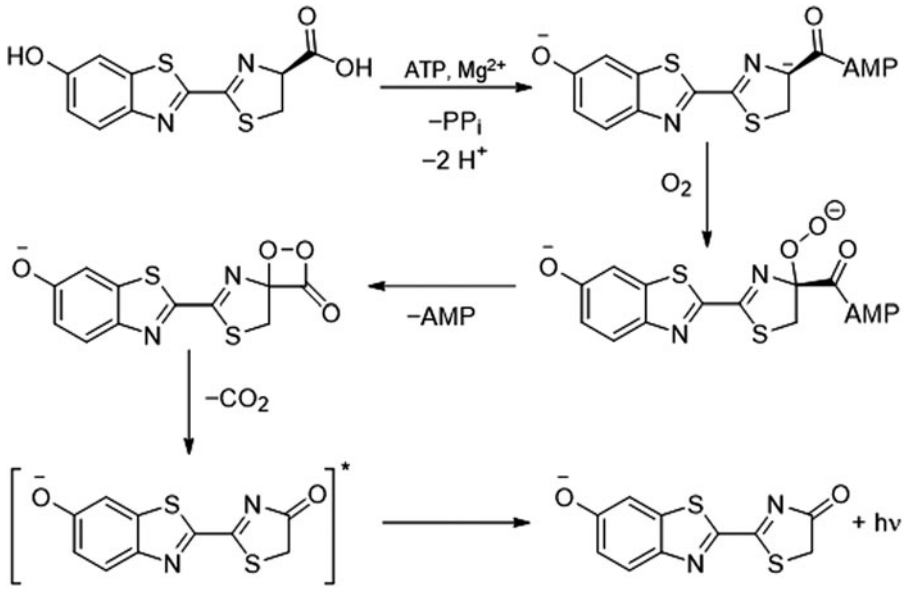

FIG. 4. General mechanism for luciferin bioluminescence.

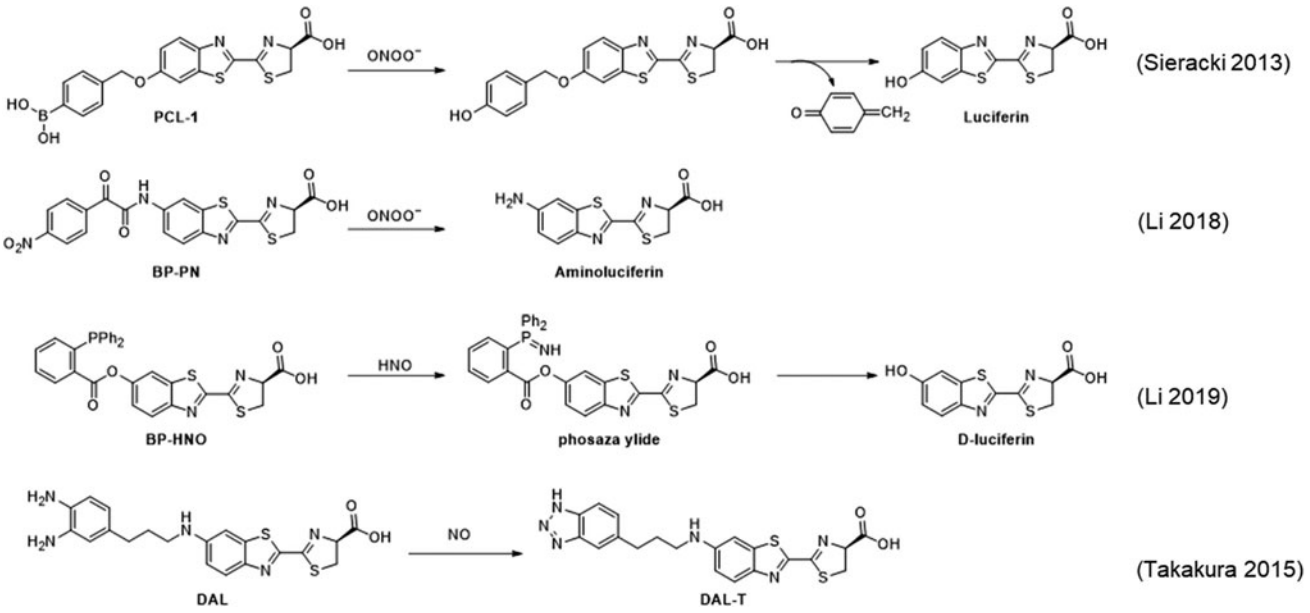

FIG. 5. Bioluminescence probes for peroxynitrite, nitroxyl, and nitric oxide.

The bioluminscent probe **BP-PN** is a caged luciferin with an α-ketoamide group that reacts with peroxynitrite to release an aminoluciferin (Fig. 5) (79). This probe was successfully used to demonstrate imaging of peroxynitrite release from SIN-1 in mouse models. For HNO, a triarylphosphine trigger that is released on a reaction with HNO *via* a phosaza ylide intermediate (104) was used to mask D-luciferin to yield the probe **BP-HNO** and enable *in vivo* bioluminescence imaging of HNO released from Angeli's salt (Fig. 5) (80).

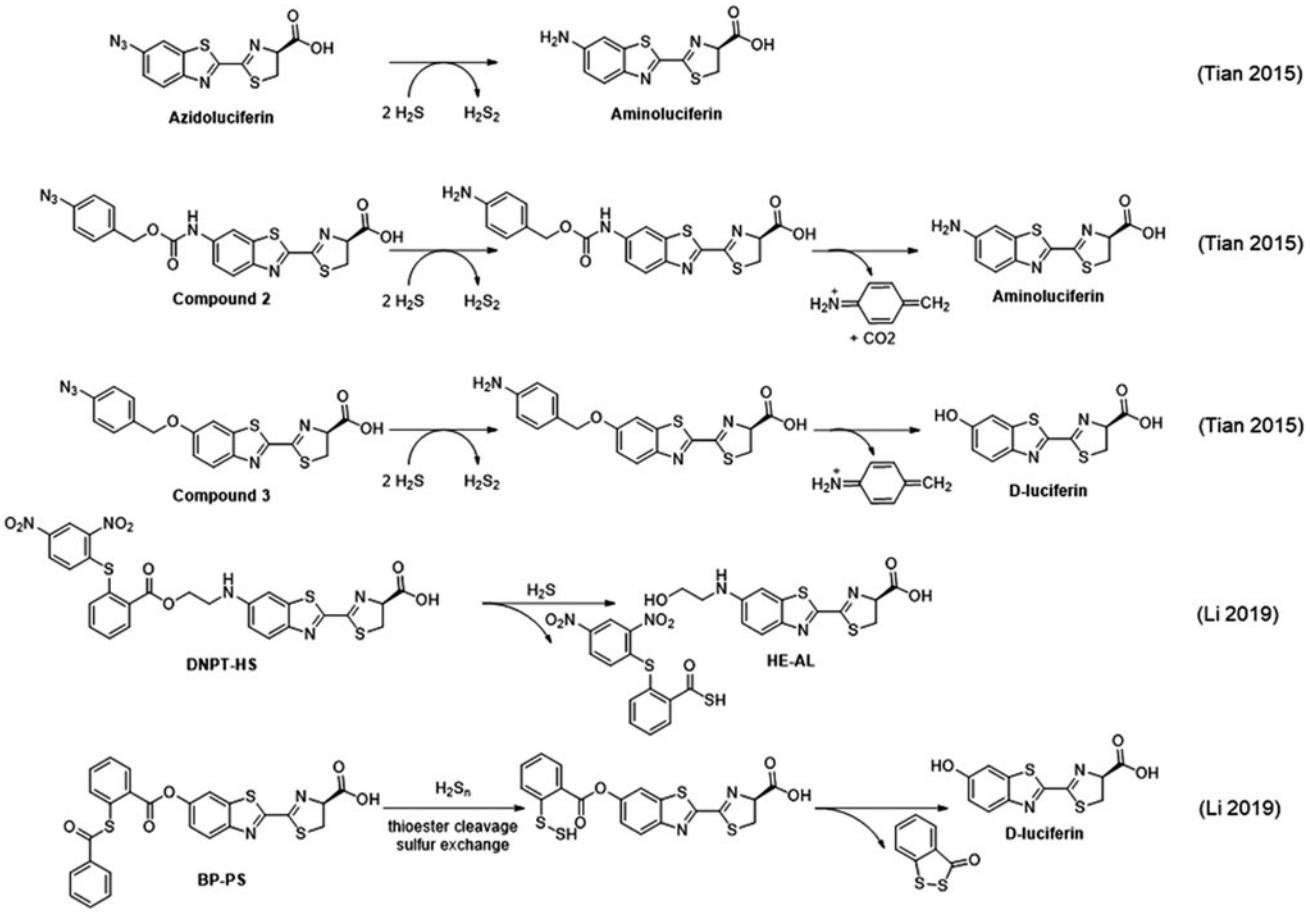

FIG. 6. Bioluminescence probes for hydrogen sulfide and polysulfide species.

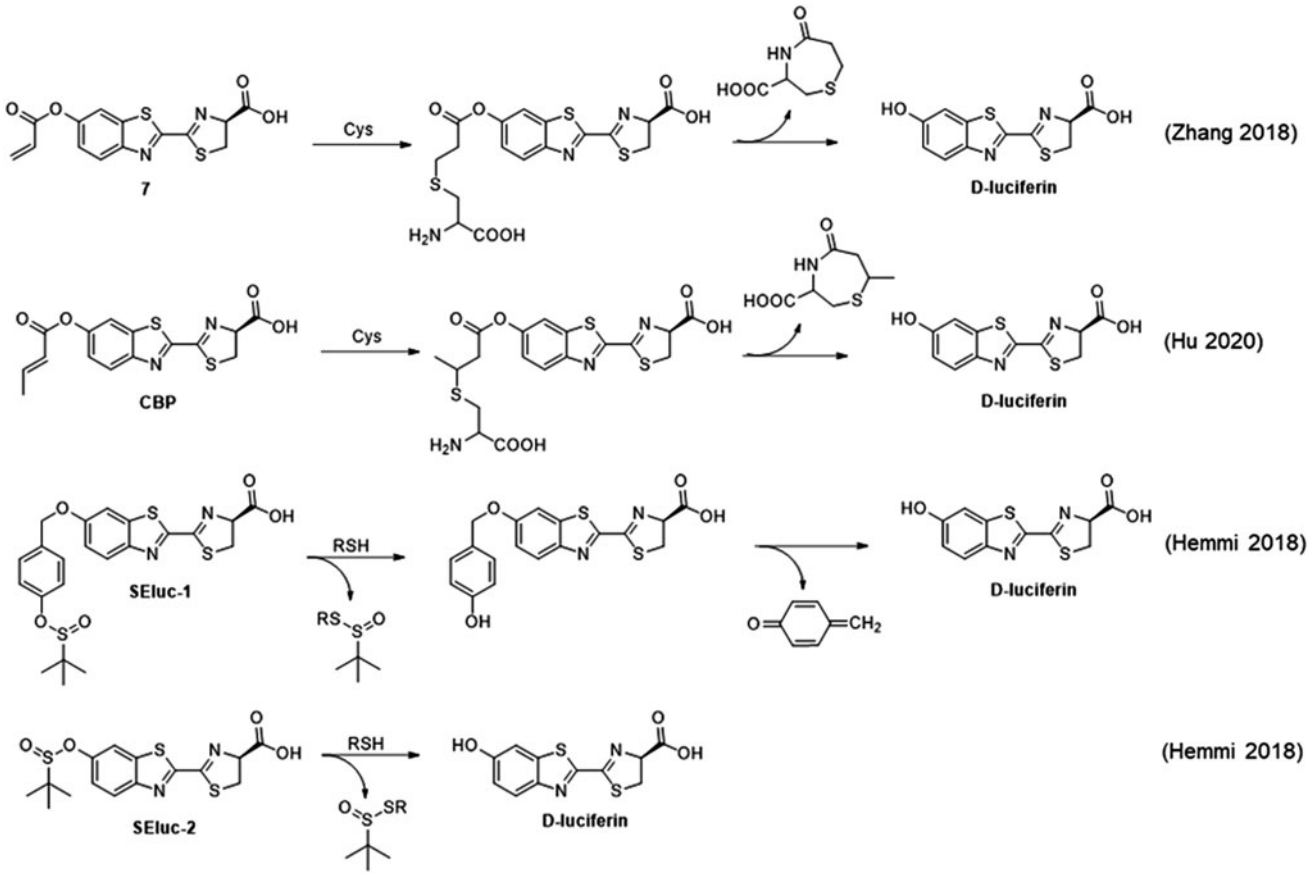

FIG. 7. Bioluminescence probes for thiols.

DAL is a bioluminescence probe for $NO^{\bullet}$ imaging (Fig. 5) (125). This probe was designed by using an interesting and innovative application of photoinduced electron transfer (PeT) quenching. Although PeT is widely used in fluorescence probes, this study applied it to use in a luciferin molecule appended with a nitric oxide reactive diamino phenyl group.

Before reacting with nitric oxide, the diamino phenyl group quenches the chemiluminescence from the enzymatically produced excited state of the luciferin derivative. After reacting with nitric oxide to form a triazole, PeT quenching is reduced and an increase in luminescence emission can be observed. This mechanism was referred to as Bioluminescent Enzyme-Induced Electron Transfer (BioLeT), and is essentially identical to PeT, accept that the transition state is accessed through a bioluminescent enzymatic reaction. This bioluminescent nitric oxide probe **DAL** was successful in imaging $NO^{\bullet}$ release from a donor molecule *in vivo*.

Bioluminescent probes for H_2S have been developed by using an azide trigger to directly release aminoluciferin, named **Azidoluciferin** (Fig. 6) (67, 126), as well as self-immolative linkers (51) to release luciferin after spontaneous elimination of the self-immolative group (Fig. 6, Compounds **2**, **3**) (67). These probes were used to image H_2S added in the form of NaSH in the whole mouse (67) and in a tumor xenograft model (126). Another strategy was implemented for the probe **DNPT-HS**, which used a dinitrothiophenol cage that released 2-hydroxyethyl luciferin (**HE-AL**) on reaction with hydrogen sulfide (82). This probe showed a decreased signal in mice treated with the broad-spectrum CBS inhibitor aminooxyacetic acid (AOAA), consistent with the observation of signals from baseline levels of hydrogen sulfide.

A bioluminescent probe for H_2S_n, **BP-PS**, was developed (81) by caging luciferin with a 2-thioester benzoate group that reacts with polysulfide species *via* a thioester cleavage reaction, followed by sulfur atom exchange (Fig. 6) (25). This study observed increases in polysulfides in *in vivo* models of inflammation, including an injection with LPS and bacterial infection.

Bioluminescent probes for cysteine have been developed by caging luciferin with an acrylate (Compound **7**, Fig. 7) (145) or methyl acrylate (**CBP**, Fig. 7) (59) group that can react with cysteine *via* conjugate addition and formation of a 7-membered caprolactam ring to release the bioluminescent substrate. These probes were shown to have an increased signal with an injection of cysteine *in vivo*. A pair of general probes for thiols was developed by incorporating a sulfinate cage on to a luciferin molecule, either directly or through a self-immolative linker (**SEluc-2** and **SEluc-1**, Fig. 7) (57). The self-immolative sulfinate **SEluc-2** had a lower background and was used to study the time-course of thiol depletion on exposing cells to oxidative stress, followed by the recovery of signals with exogenous addition of cysteine.

Chemiluminescent 1,2-Dioxetane Probes for Reactive Sulfur and Nitrogen Species

Triggered chemiluminescence from sterically hindered 1,2-dioxetanes was first accomplished by Schaap *et al.* and

these structures were soon after commercialized for *in vitro* assays (112–114). These molecules undergo a triggered chemiluminescence reaction that is believed to proceed through a chemically initiated electron exchange luminescence (CIEEL) mechanism (128), with a solvent cage mediated back electron transfer as the central excitation step (Fig. 8). Although some experimental evidence supports this mechanism, other mechanisms have been proposed and there is still debate (128).

It was only decades later when it was realized that these could actually be used for live cell experiments and *in vivo* imaging (23, 87). Soon after, key modifications of the molecular structure were developed to red-shift the emission and increase the chemiluminescence quantum yield in aqueous systems, leading to a surge of interest in these structures (53, 84). Many new biological imaging probes have now been developed (55), including chemiluminescent 1,2-dioxetane probes for reactive sulfur and nitrogen species (Figs. 9–11).

The peroxynitrite-mediated oxidative decarbonylation of an isatin (18) was used to develop an acrylonitrile 1,2-dioxetane chemiluminescence probe for peroxynitrite, called **PNCL** (Fig. 9) (22). The probe was validated by using the peroxynitrite donor compound SIN-1 in A549 epithelial lung cancer cells and RAW 264.7 macrophages and was shown to be able to detect peroxynitrite formation observed on LPS stimulation, using direct scavenging of peroxynitrite and iNOS inhibition as negative controls. This probe was further used in a study on radiation-induced erectile dysfunction (136).

PNCL was used to show that peroxynitrite was generated on exposing endothelial cells with a therapeutic dose of radiation. Further, treatment with sildenafil attenuated peroxynitrite production, suggesting that the inhibition of peroxynitrite production plays a role in how sildenafil prevents erectile dysfunction after radiation therapy.

A series of probes based on the oxidative decarbonylation of a formyl ester trigger and various 1,2-dioxetane scaffolds for the detection of peoxynitrite have been developed (60, 61). An NIR dicyanometh-ylene-4*H*-benzopyran 1,2-dioxetane scaffold was equipped with the formyl ester trigger and appended with a (2-hydroxypropyl)-β-cyclodextrin to make the renal clearable probe **NCR2** (Fig. 9). The probe was well validated and shown to have better tissue penetration than a comparable green-emitting probe. It was further used to study peroxynitrite production in a cisplatin-induced acute kidney injury model as well as providing a pharmacokinetic analysis of dioxetanes of this type.

Recently, this concept was expanded to develop a series of even more red-shifted NIR probes, **NCP$_S$** and **NCP$_{Se}$**, for peroxynitrite detection using the formyl ester trigger (Fig. 9) (61). These probes have remarkably long wavelength emissions above 750 nm by virtue of sulfur and selenium substitution of dicyanometh-ylene-4*H*-benzopyran to form a dicyanometh-ylene-4*H*-benzothiopyran and a dicyanometh-ylene-4*H*-benzoselenopyran, respectively. It was demonstrated that peroxynitrite could be detected through up to 2 cm of avian tissue, and a galactosidase variant of the NIR scaffold was used for cell and whole animal imaging.

A 1,2-dioxetane probe for HNO, **HNOCL-1**, was developed by using a triaryl phosphine HNO trigger and an acrylonitrile 1,2-dioxetane (Fig. 9) (6). A centrally important aspect of this study was the development of a kinetics-based approach that allowed quantification of the real-time dynamics of HNO production from the decomposition of Angeli's salt and the reaction between nitric oxide and hydrogen sulfide.

The relevant rate constants for the reaction of the probe with HNO and the rate-limiting step of the CIEEL mechanism were measured, and the chemiluminescence emission from the phenol scaffold was carefully calibrated. An equation was derived to convert the raw chemiluminescence emission into a concentration of HNO and used to measure picomolar concentrations of HNO generated in the reaction between hydrogen sulfide and nitric oxide. The probe was further used to detect HNO release from donor compounds in living cells and live mouse models.

An early example of detecting H_2S with a 1,2-dioxetane used a dinitrophenyl group that could release the dioxetane phenol *via* a nucleophilic aromatic substitution reaction (Compound **6**, Fig. 10) (127). A selective change in the absorbance was observed, and strong chemiluminescence emission was accomplished under alkaline conditions. **CHS-1**, **CHS-2**, and **CHS-3** use an azide-based strategy and a self-immolative carbamate linker for the chemiluminescence detection of H_2S, with the chlorine-substituted **CHS-3** being the most effective (Fig. 10) (23). This probe was used to measure H_2S production in cells supplemented with cysteine and was the first demonstration that 1,2-dioxetanes could be used for *in vivo* imaging of reactive species such as hydrogen sulfide.

CL-N3 and **CL-DNP** are another set of dioxetanes equipped with an azide or dinitrophenyl trigger and a molecular structure that is modified with an acrylonitrile group

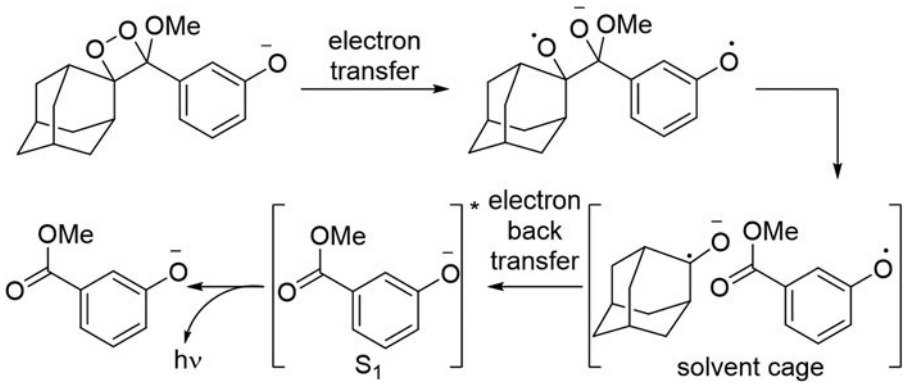

FIG. 8. CIEEL mechanism for 1,2-dioxetane chemiluminescence. CIEEL, chemically initiated electron exchange luminescence.

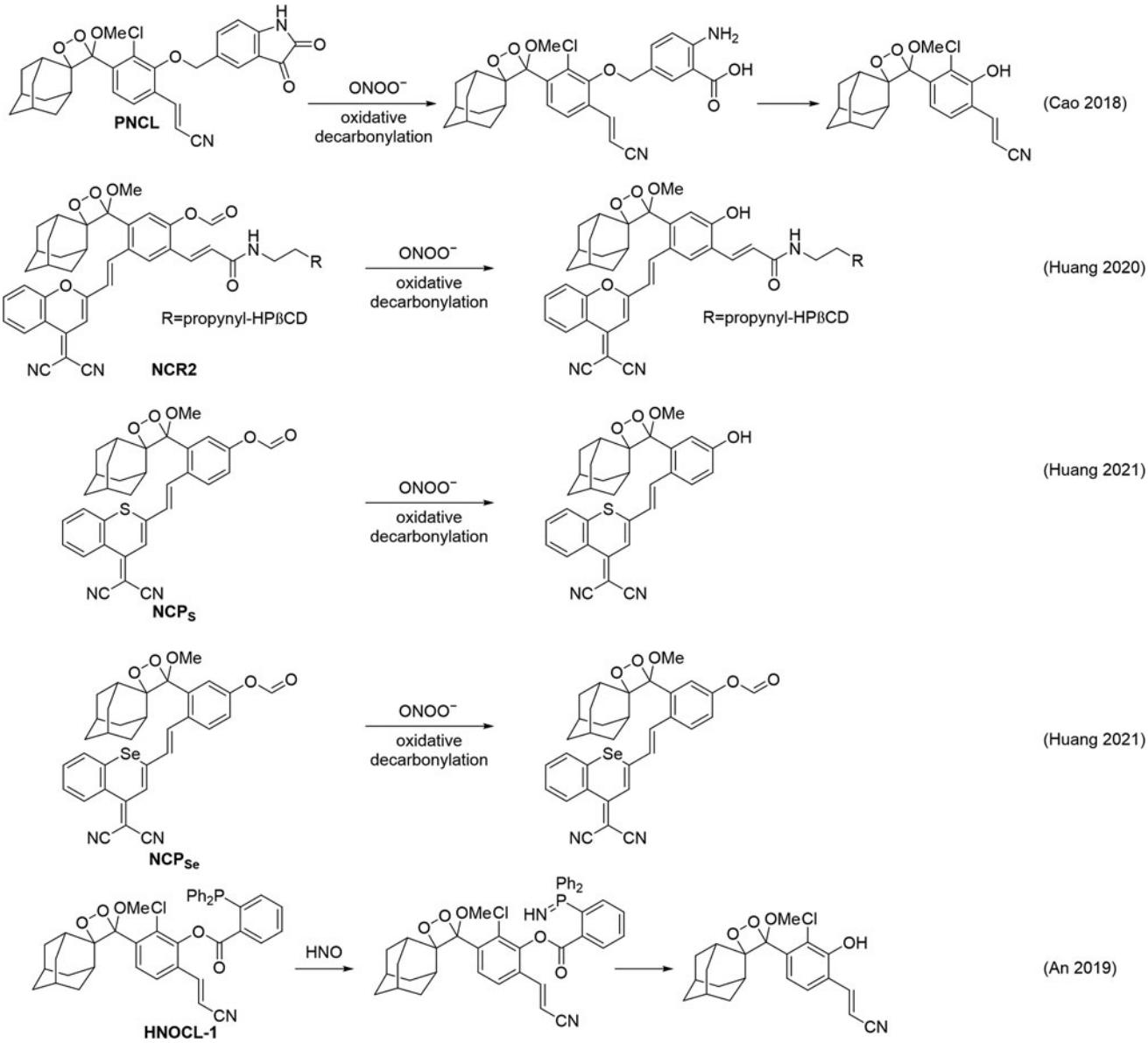

FIG. 9. 1,2-Dioxetane probes for peroxynitrite and nitroxyl.

(Fig. 10), which resulted in more efficient chemiluminescence emission in water without the need for the addition of polymers for encapsulation, enzymes to initiate the chemiluminescence reaction, or other additives (76). This study also provided a direct comparison of the sensitivity of these two triggers. Interestingly, **SCL-2**, a 1,2-dioxetane probe with a structure similar to **CL-DNP** but without a chlorine atom, was shown to be able to detect hydrogen sulfide in cells and animal (146).

A series of chemiluminescent probes for hydrogen sulfide were reported to be using a disulfide, seleno-sulfide, or dinitrosulfonyl amide trigger (Fig. 11, Probes **1**–**3**) (48). These probes were used to show the production of hydrogen sulfide in the biodegradation of β-lactam antibiotics, suggesting that hydrogen sulfide may be a useful biomarker of resistant bacteria. A 1,2-dioxetane probe for cysteine, **CL-cys**, was developed by using an acrylate trigger and appendage of a methylacrylate to the chemiluminescent core that red-shifts emission and improves chemiluminescence quantum yield (Fig. 11) (124). This probe was used to image cysteine in animal models and displayed an attenuation of signal when treating with *N*-ethylmaleimide, consistent with blocking endogenous thiol species.

Nanoparticle Chemiluminescence Approaches

There are now several examples of nanoparticle-based chemiluminescence systems that have been used for the detection and measurement of reactive sulfur and nitrogen species. Cadmium telluride (CdTe) quantum dots (147) and carbon dot nanoparticles (148) have been used for chemiluminescence peroxynitrite detection based on a proposed mechanism of generating a hydroxyl radical/superoxide radical-pair that leads to the generation of luminescence in the nanoparticles. Another carbon dot system was used for detecting nitrite by first oxidizing it to peroxynitrous acid,

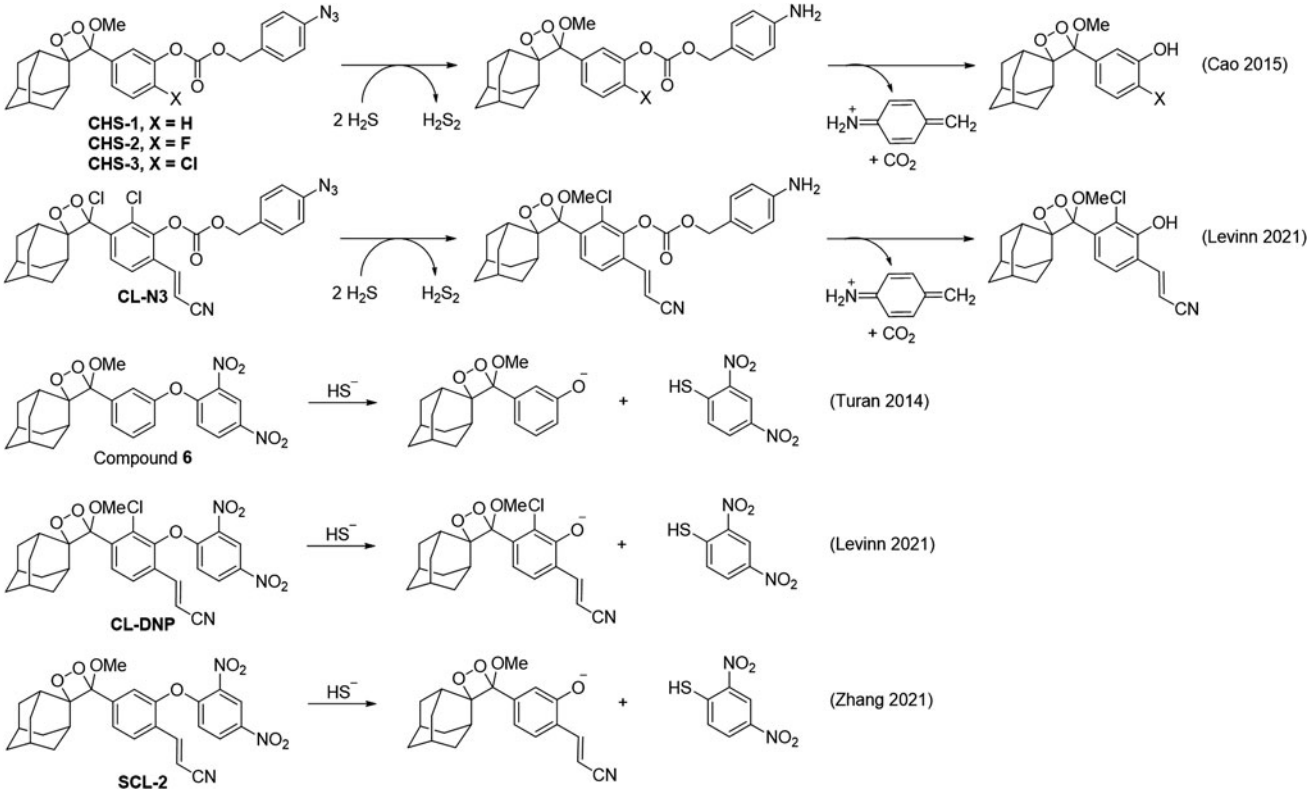

FIG. 10. 1,2-Dioxetane probes for hydrogen sulfide.

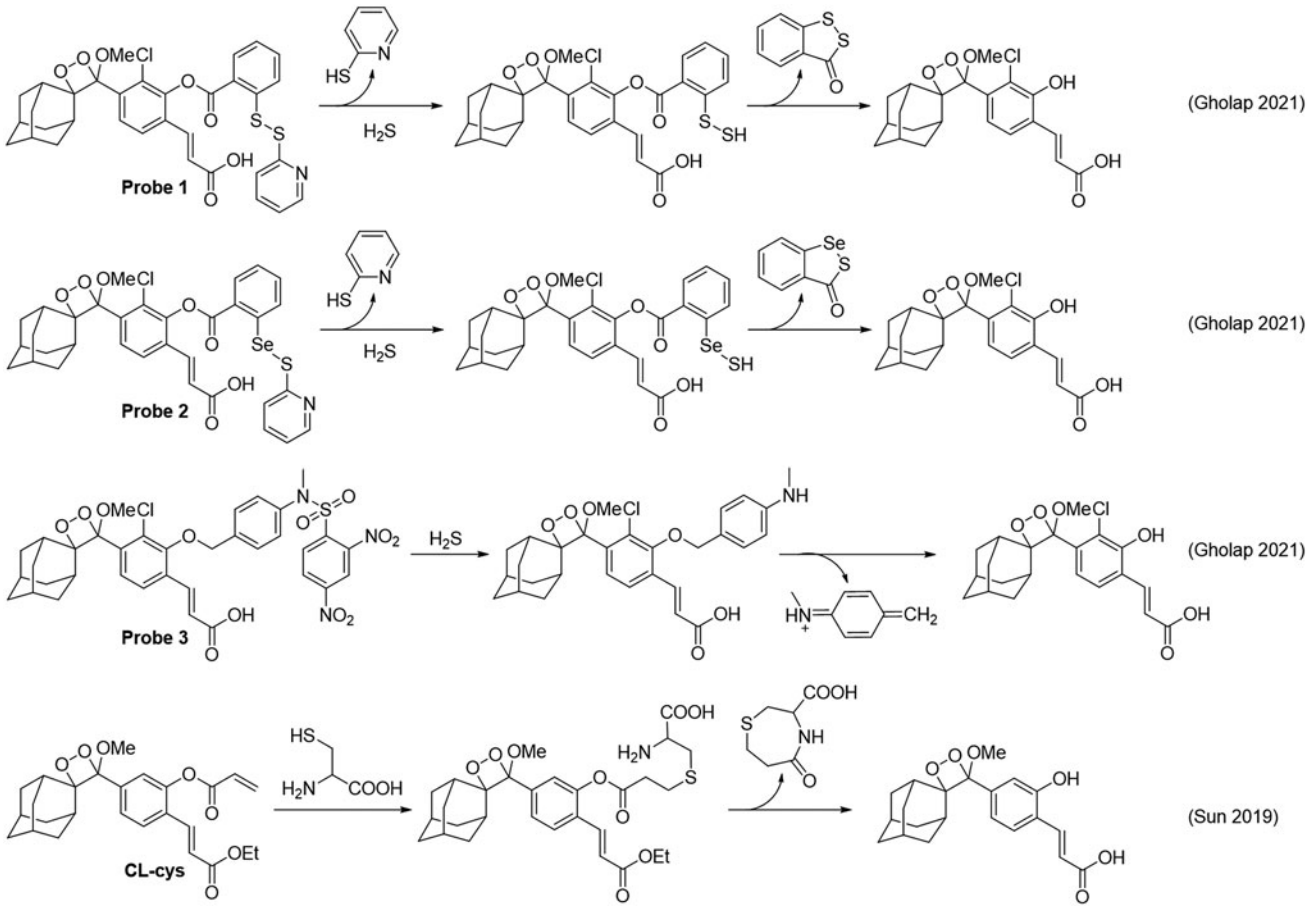

FIG. 11. 1,2-Dioxetane probes for hydrogen sulfide and cysteine.

followed by reacting with the carbon dots to initiate chemiluminescence (83). Carbon dots have also been reported to have chemiluminescence emission when treated with acidic potassium permanganate in a process that is enhanced by sulfide (85).

Nanoparticles composed of an O-pentacene molecule display chemiluminescence on reaction with peroxynitrite *via* a proposed mechanism that invokes the formation of an O-pentacene peroxide species (134). These nanoparticles were used to image peroxynitrite in several *in vivo* models and represent an emerging chemiluminescence approach for the detection of reactive sulfur and nitrogen species.

Conclusions

Chemiluminescence is a powerful approach for the detection, measurement, and imaging of reactive sulfur and nitrogen species. Ozone-based chemiluminescence is a well-established and widely adopted method for monitoring hydrogen sulfide and nitric oxide in biological systems. High selectivity and sensitivity for hydrogen sulfide can be achieved when combining ozone-based chemiluminescence detection with gas chromatography. Selectivity for nitric oxide is generally achieved by using chemical treatments that release nitric oxide from specific biological stores, block reactivity from unwanted species, and cap other biological molecules to keep them from recapturing any released nitric oxide.

Although ozone-based chemiluminescence is very well suited for sampled and homogenized tissues, it is not a viable technique for making measurements in living intact specimens due to the need to use highly reactive and toxic ozone to generate a signal. Luminol systems have also been well studied and are a useful technique for measuring reactive nitrogen species when combined with careful controls to determine which reactive species is leading to signals. Hydrogen sulfide has been measured by using an azide-caged luminol derivative and this relatively unexplored strategy may be amenable to the detection of other types of analytes. Further, *in vivo* detection of reactive nitrogen species has been accomplished by using luminol derivatives and careful control experiments to determine which species are generated during the biological process being studied.

Caging strategies have been successful in using luciferin to generate bioluminescent probes and spiroadamantane 1,2-dioxetanes to generate non-enzymatic chemiluminescent probes. A key advantage of these systems is that they can be used in living cells and animals with a selectivity that is imparted by the design of chemoselective reaction-based sensing triggers. This represents a versatile strategy that could be applied to a wide range of analytes. Bioluminescence requires genetically modified organisms, which can be an advantage or disadvantage depending on the experiment. Though quite promising, caged luciferin and dioxetanes are not as well established as ozone-based luminescence and the sensing triggers need to be carefully investigated and cross-validated.

The development of quantitative methods using ratiometric (5, 107) or kinetics-based (6, 108) approaches should further aid in the validation and general adoption of these probes. Another challenge is that most caged luciferin and dioxetane structures require complex multi-step organic synthesis, which sometimes limits their use to the group that developed the probe or close collaborators. It should be noted that 1,2-dioxetanes have been commercially available for many years, so commercialization of new molecular structures should not be an insurmountable problem.

An overview of the chemiluminescence literature brings some comparisons to light. Although ozone-based and luminol chemiluminescence have been used for measuring reactive sulfur and nitrogen species for several decades, the use of caged luciferin and 1,2-dioxetanes has only emerged in the past 10 years or so. The development of ozone-based chemiluminescence was marked by healthy scientific debate, particularly for the measurement of *S*-nitroso compounds, and eventually leads to the careful evaluation and construction of effective, reproducible methods. This has also been seen to some degree with luminol systems and select caged probes such as the bioluminescent probe **PCL-1**.

The field of caged probes, including caged luciferin and caged 1,2-dioxetanes, is largely driven by synthetic chemists. Because of this, there is often an emphasis placed on new molecular structures with brighter and red-shifted emission, sensitivity, solubility, and other molecular properties. Although these are certainly important, they often overshadow the critical need to develop rigorous quantitative methods, transparent studies of reproducibility, and cross-validation among different researchers (14). Nevertheless, given time, careful studies, and a continuation of healthy constructive debate, the prospects for using chemiluminescence for the analysis and imaging of reactive sulfur and nitrogen species in living systems are far reaching and sure to deeply impact our understanding of the roles they play in physiology and pathophysiology.

Acknowledgment

The content is solely the responsibility of the authors and does not necessarily represent the official views of the National Institutes of Health or the National Science Foundation.

Authors' Contributions

A.R.L. conceived the presented review. B.L., Y.L.K., and A.R.L. contributed to the writing of the article.

Author Disclosure Statement

A.R.L. declares a financial stake in BioLum Sciences, LLC. All other authors have no competing financial interests.

Funding Information

The authors acknowledge funding from the National Institute of General Medical Sciences of the National Institutes of Health under Award number R15GM114792-02 and the National Science Foundation under Award number CHE 1653474.

References

1. Abe K and Kimura H. The possible role of hydrogen sulfide as an endogenous neuromodulator. *J Neurosci* 16: 1066–1071, 1996.

2. Adams L, Franco MC, and Estevez AG. Reactive nitrogen species in cellular signaling. *Exp Biol Med* 240: 711–717, 2015.
3. Akaike T, Ida T, Wei FY, Nishida M, Kumagai Y, Alam MM, Ihara H, Sawa T, Matsunaga T, Kasamatsu S, Nishimura A, Morita M, Tomizawa K, Nishimura A, Watanabe S, Inaba K, Shima H, Tanuma N, Jung M, Fujii S, Watanabe Y, Ohmuraya M, Nagy P, Feelisch M, Fukuto JM, and Motohashi H. Cysteinyl-tRNA synthetase governs cysteine polysulfidation and mitochondrial bioenergetics. *Nat Commun* 8: 1177, 2017.
4. Akimoto H, Finlayson BJ, and Pitts JN, Jr. Chemiluminescent reactions of ozone with hydrogen sulphide, methyl mercaptan, dimethyl sulphide and sulphur monoxide. *Chem Phys Lett* 12: 199–202, 1971.
5. An W, Mason RP, and Lippert AR. Energy transfer chemiluminescence for ratiometric pH imaging. *Org Biomol Chem* 16: 4176–4182, 2018.
6. An W, Ryan LS, Reeves AG, Bruemmer KJ, Mouhaffel M, Gerberich J, Winters A, Mason RP, and Lippert AR. A chemiluminescent probe for HNO quantification and real-time monitoring in living cells. *Angew Chem Int Ed* 58: 1361–1365, 2019.
7. Antosova M, Morka D, Pepucha L, Plevkova J, Buday T, Serusky M, and Bencova A. Physiology of nitric oxide in the respiratory system. *Physiol Res* 66(Suppl 2): S159–S172, 2017.
8. Archer S. Measurement of nitric oxide in biological models. *FASEB J* 7: 349–360, 1993.
9. Bailey TS and Pluth MD. Chapter five—chemiluminescent detection of enzymatically produced H_2S. *Methods Enzymol* 554: 81–99, 2015.
10. Bailey TS and Pluth MD. Chemiluminescent detection of enzymatically produced hydrogen sulfide: substrate hydrogen bonding influences selectivity for H_2S over biological thiols. *J Am Chem Soc* 135: 16697–16704, 2013.
11. Basu S, Wang X, Gladwin MT, and Kim-Shapiro DB. Chemiluminescent detection of *S*-nitrosated proteins: comparison of tri-iodide, copper/CO/cysteine, and modified copper/cysteine methods. *Methods Enzymol* 440: 137–156, 2008.
12. Basudhar D, Bharadwaj G, Somasundaram V, Cheng RYS, Ridnour LA, Fujita M, Lockett SJ, Anderson SK, McVicar DW, and Wink DA. Understanding the tumor microenvironment communication network from an NOS2/COX2 perspective. *Br J Pharmacol* 176: 155–176, 2019.

12a. Beda N and Nedospasov A. A spectrophotometric assay for nitrate in an excess of nitrite. *Nitric Oxide* 13: 93–97, 2005.

13. Benner RL and Stedman DH. Universal sulfur detection by chemiluminescence. *Anal Chem* 61: 1268–1271, 1989.
14. Bezner BJ, Ryan LS, and Lippert AR. Reaction-based luminescent probes for reactive sulfur, oxygen, and nitrogen species: analytical techniques and recent progress. *Anal Chem* 92: 309–326, 2020.
15. Birks JW and Kuge MC. Chemiluminescent aerosol spray detector for liquid chromatography. *Anal Chem* 52: 897–901, 1980.
16. Braman RS and Hendrix SA. Nanogram nitrite and nitrate determination in environmental and biological materials by vanadium(III) reduction with chemiluminescence detection. *Anal Chem* 61: 2715–2718, 1989.
17. Brien JF, McLuaghlin BE, Nakatsu K, and Marks GS. Quantitation of nitric oxide formation from nitrovasodilator drugs by chemiluminescence analysis of headspace gas. *J Pharmacol Methods* 25: 19–27, 1991.
18. Bruemmer KJ, Merrikhihaghi S, Lollar CT, Morris SNS, Bauer JH, and Lippert AR. 19F magnetic resonance probes for detecting peroxynitrite in living cells using an oxidative decarbonylation reaction. *Chem Commun* 50: 12311–12314, 2014.
19. Bryan NS and Lefer DJ. Update on gaseous signaling molecules nitric oxide and hydrogen sulfide: strategies to capture their functional activity for human therapeutics. *Mol Pharmacol* 96: 109–114, 2019.
20. Bush PA, Gonzalez NE, Griscavage JM, and Ignarro LJ. Nitric oxide synthase from cerebellum catalyzes the formation of equimolar quantities of nitric oxide and citrulline from L-arginine. *Biochem Biophys Res Commun* 185: 960–966, 1992.
21. Cantrell CA, Stedman DH, and Wendel GJ. Measurement of atmospheric peroxy radicals by chemical amplification. *Anal Chem* 56: 1496–1502, 1984.
22. Cao J, An W, Reeves AG, and Lippert AR. A chemiluminescent probe for cellular peroxynitrite using a self-immolative oxidative decarbonylation reaction. *Chem Sci* 9: 2552–2558, 2018.
23. Cao J, Lopez R, Thacker JM, Moon JY, Jiang C, Morris SNS, Bauer JH, Tao P, Mason RP, and Lippert AR. Chemiluminescent probes for imaging H_2S in living animals. *Chem Sci* 6: 1979–1985, 2015.
24. Carballal S, Trujillo M, Cuevasanta E, Bartesaghi S, Möller MN, Folkes LK, García-Bereguiaín MA, Gutiérrez-Merino C, Wardman P, Denicola A, Radi R, and Alvarez B. Reactivity of hydrogen sulfide with peroxynitrite and other oxidants of biological interest. *Free Rad Biol Med* 50: 196–205, 2011.
25. Chen W, Rosser EW, Matsunaga T, Pacheco A, Akaike T, and Xian M. The development of fluorescent probes for visualizing intracellular hydrogen polysulfides. *Angew Chem Int Ed* 54: 13961–13965, 2015.
26. Clough PN and Thrush BA. Mechanism of chemiluminescent reaction between nitric oxide and ozone. *Trans Faraday Soc* 63: 915–925, 1967.
27. Clyne MAA, Thrush BA, and Wayne RP. Kinetics of the chemiluminescent reaction between nitric oxide and ozone. *Trans Faraday Soc* 60: 359–370, 1964.
28. Cortese-Krott MM, Koning A, Kuhnle GGC, Nagy P, Bianco CL, Pasch A, Wink DA, Fukuto JM, Jackson AA, van Goor H, Olson KR, and Feelisch M. The reactive species interactome: evolutionary emergence, biological significance, and opportunities for redox metabolomics and personalized medicine. *Antioxid Redox Signal* 27: 684–712, 2017.
29. Cox RD. Determination of nitrate and nitrite at the parts per billion level by chemiluminescence. *Anal Chem* 52: 332–335, 1980.
30. Daiber A, Oelze M, August M, Wendt M, Sydow K, Wiebolt H, Kleschyov AL, and Munzel T. Detection of superoxide and peroxynitrite in model systems and mitochondria by the luminol analogue L-012. *Free Radic Res* 38: 259–269, 2004.
31. DeMartino AW, Kim-Shapiro DB, Patel RP, and Gladwin MT. Nitrite and nitrate chemical biology and signalling. *Br J Pharmacol* 176: 228–245, 2019.
32. Doctor A, Platt R, Sheram ML, Eischeid A, McMahon T, Maxey T, Doherty J, Axelrod M, Kline J, Gurka M, Gow A, and Gaston B. Hemoglobin conformation couples

erythrocyte S-nitrosothiol content to O_2 gradients. *Proc Natl Acad Sci U S A* 102: 5709–5714, 2005.
33. Dóka É, Pader I, Bíro A, Johansson K, Cheng Q, Ballagó K, Prigge JR, Pastor-Flores D, Dick TP, Schmidt EE, Arnér ESJ, and Nagy P. A novel persulfide detection method reveals protein persulfide- and polysulfide-reducing functions of thioredoxin and glutathione systems. *Sci Adv* 2: e1500968, 2016.
34. Evangelista AM, Kohr MJ, and Murphy E. *S*-nitrosylation: specificity, occupancy, and interaction with other post-translational modifications. *Antioxid Redox Signal* 19: 1209–1219, 2013.
35. Ewing JF and Janero DR. Specific S-nitrosothiol thionitrite. quantification as solution nitrite after vanadium(III) reduction and ozone-chemiluminescent detection. *Free Radic Biol Med* 25: 621–628, 1998.
36. Fang K, Ragsdale NV, Carey RM, MacDonald T, and Gaston B. Reductive assays for *S*-nitrosotiols: implications for measurements in biological systems. *Biochem Biophys Res Commun* 252: 535–540, 1998.
37. Farah C, Michel LYM, and Balligand JL. Nitric oxide signalling in cardiovascular health and disease. *Nat Rev Cardiol* 15: 292–316, 2018.
38. Ferrer-Sueta G, Campolo N, Trujillo M, Bartesaghi S, Carballal S, Romero N, Alvarez B, and Radi R. Biochemistry of peroxynitrite and protein nitration. *Chem Rev* 118: 1338–1408, 2018.
39. Filipovic MR, Zivanovic J, Alvarez B, and Banerjee R. Chemical biology of H_2S signaling through persulfidation. *Chem Rev* 118: 1253–1337, 2018.
40. Francis SH, Busch JL, and Corbin JD. cGMP-dependent protein kinases and cGMP phosphodiesterases in nitric oxide and cGMP action. *Pharmacol Rev* 62: 525–563, 2010.
41. Fukuto J. A recent history of nitroxyl chemistry, pharmacology and therapeutic potential. *Br J Pharmacol* 176: 135–146, 2019.
42. Furne J, Saeed A, and Levitt MD. Whole tissue hydrogen sulfide concentrations are orders of magnitude lower than presently accepted values. *Am J Physiol Regul Integr Comp Physiol* 295: R1479–R1485, 2008.
43. Furne JK, Springfield J, Koenig T, Suarez F, and Levitt MD. Measurement of fecal sulfide using gas chromatography and a sulfur chemiluminescence detector. *J Chromatogr B* 754: 253–258, 2001.
44. Garai D, Ríos-González BB, Furtmüller PG, Fukuto JM, Xian M, López-Garriga J, Obinger C, and Nagy P. Mechanisms of myeloperoxidase catalyzed oxidation of H_2S by H_2O_2 or O_2 to produce potent protein Cys-polysulfide-inducing species. *Free Radic Biol Med* 113: 551–563, 2017.
45. Garside C. A chemiluminescent technique for the determination of nanomolar concentrations of nitrate and nitrite in seawater. *Mar Chem* 11: 159–167, 1982.
46. Garthwaite J. NO as a multimodal transmitter in the brain: discovery and current status. *Br J Pharmacol* 176: 197–211, 2019.
47. Gaydon AG. Spectrum of the afterglow of sulphur dioxide. *Proc Roy Soc* A 146: 901–910, 1934.
48. Gholap SP, Yao C, Green O, Babjak M, Jakubed P, Malatinkský T, Ihssen J, Wick L, Spitz U, and Shabat D. Chemiluminescence detection of hydrogen sulfide release by β-lactamase-catalyzed β-lactam biodegradation: unprecedented pathway for monitoring β-lactam antiobiotic bacterial resistance. *Bioconjugate Chem* 35: 991–1000, 2021.
49. Glinski RJ, Sedarski JA, and Dixon DA. Single-collision chemiluminescent reactions of ozone with hydrogen sulfide and methyl mercaptan. *J Am Chem Soc* 104: 1126–1128, 1982.
50. Glinski RJ, Sedarski JA, and Dixon DA. The chemiluminescent reaction of ozone with methyl mercaptan. *J Phys Chem* 85: 2440–2443, 1981.
51. Gnaim S and Shabat D. Activity-based optical sensing enabled by self-immolative scaffolds: monitoring of release events by fluorescence or chemiluminescence output. *Acc Chem Res* 53: 2806–2817, 2019.
52. Greaves JC and Garvin D. Chemically induced molecular excitation: excitation spectrum of the nitric oxide-ozone system. *J Chem Phys* 30: 348–349, 1959.
53. Green O, Eilon T, Hananya N, Gutkin S, Bauer CR, and Shabat D. Opening a gateway for chemiluminescence cell imaging: distinctive methodology for design of bright chemiluminescent dioxetane probes. *ACS Cent Sci* 3: 349–358, 2017.
54. Halstead CJ and Thrush BA. The kinetics of elementary reactions involving the oxides of sulphur III. The chemiluminescent reaction between sulphur monoxide and ozone. *Proc Roy Soc* A 295: 380–398, 1966.
55. Hananya N and Shabat D. Recent advances and challenges in luminescent imaging: bright outlook for chemiluminescence of dioxetanes in water. *ACS Cent Sci* 5: 949–959, 2019.
56. Heinrich TA, da Silva RS, Miranda KM, Switzer CH, Wink DA, and Fukuto JM. Biological nitric oxide signalling: chemistry and terminology. *Br J Pharmacol* 169: 1417–1429, 2013.
57. Hemmi M, Ikeda Y, Sindo Y, Nakajima T, Nishiyama S, Oka K, Sato M, Hiruta Y, Citterio D, and Suzuki K. Highly sensitive bioluminescent probe for thiol detection in living cells. *Chem Asian J* 13: 648–655, 2018.
58. Hendgen-Cotta U, Grau M, Rassaf T, Gharini P, Kelm M, and Kleinbongard P. Chapter sixteen—reductive gas-phase chemiluminescence and flow injection analysis for measurement of the nitric oxide pool in biological matrices. *Methods Enzymol* 441: 295–315, 2008.
59. Hu S, Li P, Zhou S, Kang T, Hai A, Ma Y, Liu Y, Ke B, and Li M. Bioluminescence imaging of exogenous & endogenous cysteine in vivo with a highly selective probe. *Bioorg Med Chem Lett* 30: 126968, 2020.
60. Huang J, Huang J, Cheng P, Jiang Y, and Pu K. Near-infrared chemiluminescent reporters for in vivo imaging of reactive oxygen and nitrogen species in kidneys. *Adv Funct Mater* 30: 2003628, 2020.
61. Huang J, Jiang Y, Li J, Huang J, and Pu K. Molecular chemiluminescent probes with a very long near-infrared emission wavelength for in vivo imaging. *Angew Chem Int Ed* 60: 3999–4003, 2021.
62. Ida T, Sawa T, Ihara H, Tsuchiya Y, Watanabe Y, Kumagai Y, Suematsu M, Motohashi H, Fujii S, Matsunaga T, Yamamoto M, Ono K, Devarie-Baez NO, Xian M, Fukuto JM, and Akaike T. Reactive cysteine persulfides and S-polythiolation regulate oxidative stress and redox signaling. *Proc Natl Acad Sci U S A* 111: 7606–7611, 2014.
63. Ignarro LJ. Nitric oxide is not just blowing in the wind. *Br J Pharmacol* 176: 131–134, 2019.
64. Ivanovic-Burmazovic I and Filipovic MR. Saying NO to H_2S: a story of HNO, HSNO, and $SSNO^-$. *Inorg Chem* 58: 4309–4051, 2019.

65. Kabil O and Banerjee R. Enzymology of H_2S biogenesis, decay and signaling. *Antioxid Redox Signal* 20: 770–782, 2014.
66. Kabil O, Vivitsky V, Xie P, and Banerjee R. The quantitative significance of the transulfuration enzymes for H_2S production in murine tissues. *Antioxid Redox Signal* 15: 363–372, 2011.
67. Ke B, Wu W, Liu W, Liang H, Gong D, Hu X, and Li M. Bioluminescence probe for detecting hydrogen sulfide in vivo. *Anal Chem* 88: 592–595, 2016.
68. Kelly TJ, Spicer CW, and Ward GF. An assessment of the luminol chemiluminescence technique for measurement of NO_2 in ambient air. *Atmos Environ* 24A: 2397–240, 1990.
69. Kielland A, Blom T, Nandakumar KS, Holmdahl R, Blomhoff, and Carlsen H. In vivo imaging of reactive oxygen and nitrogen species in inflammation using the luminescent probe L-012. *Free Radic Biol Med* 47: 760–766, 2009.
70. Kikuchi K, Nagano T, Hayakawa H, Hirata Y, and Hirobe M. Detection of nitric oxide production from a perfused organ by a luminol-H_2O_2 system. *Anal Chem* 65: 1794–1799, 1993.
71. Kimura H. Hydrogen sulfide: from brain to gut. *Antioxid Redox Signal* 12: 1111–1123, 2010.
72. King AL, Polhemus DJ, Bhusan S, Otsuka H, Kondo K, Nicholson CK, Bradley JM, Islam KN, Calvert JW, Tao YX, Dugas TR, Kelley EE, Elrod JW, Huang PL, Wang R, and Lefer DJ. Hydrogen sulfide cytoprotective signaling is endothelial nitric oxide synthase-nitric oxide dependent. *Proc Natl Acad Sci U S A* 111: 3182–3187, 2014.
73. Kolluru G, Shen X, and Kevil CG. Reactive sulfur species: a new redox player in cardiovascular pathophysiology. *Arterioscler Thromb Vasc Biol* 40: 874–884, 2020.
74. Kummer WA, Pitts JN, and Steer RP. Chemiluminescent reactions of ozone with olefins and sulfides. *Environ Sci Technol* 5: 1045–1047, 1971.
75. Lau N and Pluth MD. Reactive sulfur species (RSS): persulfides, polysulfides, potential, and problems. *Curr Opin Chem Biol* 49: 1–8, 2019.
76. Levinn CM and Pluth MD. Direct comparison of triggering motifs on chemiluminescent probes for hydrogen sulfide detection in water. *Sens Actuator B Chem* 329: 129235, 2021.
77. Levitt MD, Abel-Rehim MS, and Furne J. Free and acid-labile hydrogen sulfide concentrations in mouse tissues: anomalously high free hydrogen sulfide in aortic tissue. *Antioxid Redox Signal* 15: 373–378, 2011.
78. Levitt MD, Furne J, Springfield J, Suarez F, and DeMaster E. Detoxification of hydrogen sulfide and methanethiol in the cecal mucosa. *J Clin Invest* 104: 1107–1114, 1999.
79. Li JB, Chen L, Wang, Q, Liu HW, Hu XX, Yuan L, and Zhang XB. A bioluminescent probe for imaging endogenous peroxynitrite in living cells and mice. *Anal Chem* 90: 4167–4173, 2018.
80. Li JB, Wang Q, Liu HW, Yin X, Hu XX, Yuan L, and Zhang XB. Engineering of a bioluminescent probe for imaging nitroxyl in live cells and mice. *Chem Commun* 55: 1758–1761, 2019.
81. Li JB, Wang Q, Liu HW, Yuan L, and Zhang XB. A bioluminescent probe for imaging endogenous hydrogen polysulfides in live cells and a murine model of bacterial infection. *Chem Commun* 55: 4487–4490, 2019.
82. Li X, Wang A, Wang J, and Lu J. Efficient strategy for the synthesis and modification of 2-hydroxyethylluciferin for highly sensitive bioluminescence imaging of endogenous hydrogen sulfide in cancer cells and nude mice. *Anal Chem* 91: 15703–15708, 2019.
83. Lin Z, Xue W, Chen H, and Lin JM. Peroxynitrous-acid-induced chemiluminescence of fluorescent carbon dots for nitrite sensing. *Anal Chem* 83: 8245–8251, 2011.
84. Lippert AR. Unlocking the potential of chemiluminescence imaging. *ACS Cent Sci* 3: 269–271, 2017.
85. Liu B and Han S. Determination of trace hydrogen sulfide by using the permanganate induced chemiluminescence of carbon dots. *Microchim Acta* 183: 3087–3092, 2016.
86. Liu H, Radford MN, Yang CT, Chen W, and Xian M. Inorganic hydrogen polysulfides: chemistry chemical biology and detection. *Br J Pharmacol* 176: 616–627, 2019.
87. Liu L and Mason RP. Imaging beta-galactosidase activity in human tumor xenografts and transgenic mice using a chemiluminescent substrate. *PLoS One* 5: e12024, 2010.
88. MacArthur PH, Shiva S, and Gladwin MT. Measurement of circulating nitrite and *S*-nitrosothiols by reductive chemiluminescence. *J Chromatogr B* 851: 93–105, 2007.
89. Mack J and Bolton JR. Photochemistry of nitrite and nitrate in aqueous solution: a review. *J Photochem Photobiol A* 128: 1–13, 1999.
90. Maeda Y, Aoki K, and Munemori M. Chemiluminescence method for the determination of nitrogen dioxide. *Anal Chem* 52: 307–311, 1980.
91. Marley R, Feelisch M, Holt S, and Moore K. A chemiluminescence-based assay for S-nitrosoalbumin and other plasma S-nitrosothiols. *Free Radic Res* 32: 1–9, 2000.
92. McMahon TJ, Moon RE, Luschinger BP, Carraway MS, Stone AE, Stolp BW, Gow AJ, Pawloski JR, Watke P, Single DJ, Piantadosi CA, and Stamler JS. Nitric oxide in the human respiratory cycle. *Nat Med* 8: 711–717, 2002.
93. Menon NK, Pataricza J, Binder T, and Bing RJ. Reduction of biological effluents in purge and trap micro reaction vessels and detection of endothelium-derived nitric oxide (edno) by chemiluminescence. *J Mol Cell Cardiol* 23: 389–393, 1991.
94. Mishalanie EA and Birks JW. Selective detection of organosulfur compounds in high-performance liquid chromatograph. *Anal Chem* 58: 918–923, 1986.
95. Mukosera GT, Liu T, Ahmed ASI, Li Q, Sheng MHC, Tipple TE, Baylink DJ, Power GG, and Blood AB. Detection of dinitrosyl iron complexes by ozone-based chemiluminescence. *Nitric Oxide* 79: 57–67, 2018.
96. Nagababu E, Ramasamy S, Abernethy DR, and Rifkind JM. Active nitric oxide produced in the red cell under hypoxic conditions by deoxyhemoglobin-mediated nitrite reduction. *J Biol Chem* 47: 46349–46356, 2003.
97. Nagahara N, Koike S, Nirasawa T, Kimura H, and Ogasawara Y. Alternative pathway of H_2S and polysulfides production from sulfurated catalytic-cysteine of reaction intermediates of 3-mercaptopyruvate sulfurtransferase. *Biochem Biophys Res Commun* 496: 648–653, 2018.
98. Nishinaka Y, Aramaki Y, Yoshida H, Masuya H, Sugawara T, and Ichimori Y. A new sensitive chemiluminescence probe, L-012, for measuring the production of superoxide anion by cells. *Biochem Biophys Res Commun* 193: 554–559, 1993.
99. Olson KR, Gao Y, Arif F, Arora K, Patel S, DeLeon ER, Sutton TR, Feelisch M, Cortese-Krott MM, and Straub KD. Metabolism of hydrogen sulfide (H_2S) and production of reactive sulfur species (RSS) by superoxide dismutase. *Redox Biol* 15: 74–85, 2018.

100. Palmer RMJ, Ferrige AG, and Moncada S. Nitric-oxide release accounts for the biological-activity of endothelium-derived relaxing factor. *Nature* 327: 524–526, 1987.
101. Predmore BL and Lefer DJ. Development of hydrogen sulfide-based therapeutic for cardiovascular disease. *J Cardiovasc Transl Res* 3: 487–498, 2010.
102. Prolo C, Rios N, Piacenza L, Álvarez MN, and Radi R. Fluorescence and chemiluminescence approaches for peroxynitrite detection. *Free Radic Biol Med* 128: 59–68, 2018.
103. Radi R, Cosgrove TP, Beckman JS, and Freeman BA. Peroxynitrite-induced luminol chemiluminescence. *Biochem J* 290: 51–57, 1993.
104. Reisz JA, Klorig EB, Wright MW, and King SB. Reductive phosphine-mediated ligation of nitroxyl (HNO). *Org Lett* 11: 2719–2721, 2009.
105. Ritz T, Salsman ML, Young DA, Lippert AR, Khan DA, and Ginty AT. Booting nitric oxide in stress and respiratory infection: potential relevance for asthma and COVID-19. *Brain Behav Immun* 14: 100255, 2021.
106. Robinson JK, Bollinger MJ, and Birks JW. Luminol/H_2O_2 chemiluminescence detector for the analysis of nitric oxide in exhaled breath. *Anal Chem* 71: 5131–5136, 1999.
107. Ryan LS, Gerberich J, Haris U, Nguyen D, Mason RP, and Lippert AR. Ratiometric pH imaging using a 1,2-dioxetane chemiluminescence resonance energy transfer sensor in live animals. *ACS Sens* 5: 2925–2932, 2020.
108. Ryan LS, Gerberich JL, Cao J, An W, Jenkins BA, Mason RP, and Lippert AR. Kinetics-based measurement of hypoxia in living cells and animals using an acetoxymethyl ester chemiluminescent probe. *ACS Sens* 4: 1391–1398, 2019.
109. Ryan LS and Lippert AR. Ultrasensitive chemiluminescent detection of cathepsin B: insights into the new frontier of chemiluminescent imaging. *Angew Chem Int Ed* 57:622–624, 2018.
110. Samouilov A and Zweier JL. Development of chemiluminescence-based methods for specific quantitation of nitrosylated thiols. *Anal Biochem* 258: 322–330, 1998.
111. Saville B. A scheme for the colorimetric determination of microgram amounts of thiols. *Analyst* 83: 670–672, 1958.
112. Schaap AP, Chen TS, Handley RS, DeSilva R, and Giri BP. Chemical and enzymatic triggering of 1,2-dioxetanes. 2: fluoride-induced chemiluminescence from *tert*-butyldimethylsilyloxy-substituted dioxetanes. *Tetrahedron Lett* 28: 1155–1158, 1987.
113. Schaap AP, Handley RS, and Giri BP. Chemical and enzymatic triggering of 1,2-dioxetanes. 1: Aryl esterase-catalyzed chemiluminescence from a naphthyl acetate-substituted dioxetane. *Tetrahedron Lett* 28: 935–938, 1987.
114. Schaap AP, Sandison MD, and Handley RS. Chemical and enzymatic triggering of 1,2-dioxetanes. 3: Alkaline phosphatase-catalyzed chemiluminescence from an aryl phosphate-substituted dioxetane. *Tetrahedron Lett* 28: 1159–1162, 1987.
115. Schurath U, Weber M, and Becker KH. Electronic spectrum and structure of the HSO radical. *J Chem Phys* 67: 110–119, 1977.
116. Shearer RL. Development of flameless sulfur chemiluminescence detection: application to gas chromatography. *Anal Chem* 64: 2192–2196, 1992.
117. Shearer RL, O'Neal DL, Rios R, and Baker MD. Analysis of sulfur compounds by capillary column gas chromatography with sulfur chemiluminescence detection. *J Chromatogr* 28: 24–28, 1990.
118. Sieracki NA, Gantner BN, Mao M, Horner JH, Ye RD, Malik AB, Newcomb ME, and Bonini MG. Bioluminescent detection of peroxynitrite with a boronic acid-caged luciferin. *Free Radic Biol Med* 61: 40–50, 2013.
119. Stamler JS, Jaraki O, Osborne J, Simon DI, Keaney J, Vita J, Singel D, Valeri CR, and Loscalzo J. Nitric oxide circulates in mammalian plasma primarily as an *S*-nitroso adduct of serum albumin. *Proc Natl Acad Sci U S A* 89: 7674–7677, 1992.
120. Stuehr DJ and Haque MM. Nitric oxide synthase enzymology in the 20 years after the Nobel Prize. *Br J Pharmacol* 176: 177–178, 2019.
121. Su TA, Bruemmer KJ, and Chang CJ. Caged luciferins for bioluminescent activity-based sensing. *Curr Opin Biotechnol* 60: 198–204, 2019.
122. Su Y, Song H, and Lv Y. Recent advances in chemiluminescence for reactive oxygen species and imaging analysis. *Microchem J* 146: 83–97, 2019.
123. Suarez FL, Furne J, Springfield J, and Levitt MD. Production and elimination of sulfur-containing gases in the rat colon. *Am J Physiol* 274: G727–G733, 1998.
124. Sun J, Hu Z, Zhang S, and Zhang X. A novel chemiluminescent probe based on 1,2-dioxetane scaffold for imaging cysteine in living mice. *ACS Sens* 4: 87–92, 2019.
125. Takakura H, Kojima R, Kamiya M, Kobayashi E, Komatsu T, Ueno T, Terai T, Hanaoka K, Nagano T, and Urano Y. New class of bioluminogenic probe based on Bioluminescent Enzyme-Induced Electron Transfer: Bio-LeT. *J Am Chem Soc* 137: 4010–4013, 2015.
126. Tian X, Li Z, Lau C, and Lu J. Visualization of in vivo hydrogen sulfide production by a bioluminescence probe in cancer cells and nude mice. *Anal Chem* 87: 11325–11331, 2015.
127. Turan IS and Sozmen F. A chromogenic dioxetane chemosensor for hydrogen sulfide and pH dependent off–on chemiluminescence property. *Sens Actuator B Chem* 201: 13–18, 2014.
128. Vacher M, Galaván F, Ding BW, Schramm S, Berraud-Pache R, Naumov P, Ferré N, Liu YJ, Navizet I, Roca-Sanjuán D, Baader WJ, and Lindh R. Chem- and bioluminescence of cyclic peroxide. *Chem Rev* 118: 6927–6974, 2018.
129. Van de Bittner GC, Bertozzi CR, and Chang CJ. Strategy for dual-analyte luciferin imaging: in vivo bioluminescence detection of hydrogen peroxide and caspase activity in a murine model of acute inflammation. *J Am Chem Soc* 135: 1783–1795, 2013.
130. Van de Bittner GC, Dubikovskaya EA, Bertozzi CR, and Chang CJ. In vivo imaging of hydrogen peroxide production in a murine tumor model with a chemoselective bioluminescent reporter. *Proc Natl Acad Sci U S A* 107: 21316–21321, 2010.
131. Vitvitsky V and Banerjee R. Chapter seven—H_2S analysis in biological samples using gas chromatography with sulfur chemiluminescence detection. *Methods Enzymol* 554: 111–123, 2015.
132. Vivitsky V, Kabil O, and Banerjee R. High turnover rates for hydrogen sulfide allow for rapid regulation of its tissue concentrations. *Antioxid Redox Signal* 17: 22–31, 2012.

133. Wallace JL. Nitric oxide in the gastrointestinal tract: opportunities for drug development. *Br J Pharmacol* 176: 147–154, 2019.
134. Wang B, Wang Y, Wang Y, Zhao Y, Yang C, Zeng Z, Huan S, Song G, and Zhang X. Oxygen-embedded pentacene based near-infrared chemiluminescent nanoprobe for highly selective and sensitive visualization of peroxynitrite in vivo. *Anal Chem* 92: 4154–4163, 2020.
135. Wendel GJ, Stedman DH, and Cantrell CA. Luminol-based nitrogen dioxide detector. *Anal Chem* 55: 937–940, 1983.
136. Wortel RC, Mizrachi A, Li H, Markovsky E, Enyedi B, Jacobi J, Brodsky O, Cao J, Lippert AR, Incrocci L, Mulhall JP, and Haimovitz-Friedman A. Sildenafil protects endothelial cells from radiation-induced oxidative stress. *J Sex Med* 16: 1721–1733, 2019.
137. Xia H, Li Z, Sharp TE, Polhemus DJ, Carnal J, Moles KH, Tao YX, Elrod J, Pfeilschifter J, Beck KF, and Lefer DJ. Endothelial cell cystathionine γ-lyase expression level modulates exercise capacity, vascular function, and myocardial ischemia reperfusion injury. *J Am Heart Assoc* 9: e017544; 2020.
138. Yadav PK, Vitvitsky V, Kim H, White A, Cho US, and Banerjee R. S-4-Carboxyl-L-cysteine specifically inhibits cystathionine g-lyase-dependent hydrogen sulfide synthesis CSE inhibition by S-3-carboxpropy-L-cysteine. *J Biol Chem* 294: 11011–11022, 2019.
139. Yan X. Detection by ozone-induced chemiluminescence in chromatography. *J Chromatogr* 842: 267–308, 1999.
140. Yan X. Sulfur and nitrogen chemiluminescence detection in gas chromatographic analysis. *J Chromatogr* 976: 3–10, 2002.
141. Yan X. Unique selective detectors for gas chromatography: nitrogen and sulfur chemiluminescence detectors. *J Sep Sci* 29: 1931–1945, 2006.
142. Yuan S, Shen X, and Kevil CG. Beyond the gasotransmitter: hydrogen sulfide and polysulfide in cardiovascular health and immune response. *Antioxid Redox Signal* 27: 634–653, 2017.
143. Zafirou OC and McFarland M. Determination of trace levels of nitric oxide in aqueous solution. *Anal Chem* 52: 1662–1667, 1980.
144. Zhan Z, Dai Y, Li Q, and Lv Y. Small molecule-based bioluminescence and chemiluminescence probes for sensing and imaging reactive species. *TRAC-Trend Anal Chem* 134: 116129, 2021.
145. Zhang M, Wang L, Zhao Y, Wang F, Wu J, and Liang G. Using bioluminescence turn-on to detect cysteine in vitro and in vivo. *Anal Chem* 90: 4951–4954, 2018.
146. Zhang Z, Lin Y, Li Z, Dong G, Gao Y, Ma S, Li J, Du L, and Li M. Bright chemiluminescent dioxetane probes for the detection of gaseous transmitter H_2S. *Biorganic Med Chem Lett* 46: 128148, 2021.
147. Zhou W, Cao Y, Sui D, and Lu C. Radical pair-drive luminescence of quantum dots for specific detection of peroxynitrite in living cells. *Anal Chem* 88: 2659–2665, 2016.
148. Zhou W, Dong S, Lin Y, and Lu C. Insights into the role of nanostructure in the sensing properties of carbon nanodots for improved sensing of reactive oxygen species in living cells. *Chem Commun* 53: 2122–2125, 2017.
149. Zielonka J, Lambeth JD, and Kalyanaraman B. On the use of L-012, a luminol-based chemiluminescent probe, for detecting superoxide and identifying inhibitors of NADH oxidase: a re-evaluation. *Free Radic Biol Med* 65: 1310–1314, 2013.
150. Zielonka J, Podsiadly R, Zielonka M, Hardy M, and Kalyanaraman B. On the use of peroxy-caged luciferin (PCL-1) probe for bioluminescent detection of inflammatory oxidants in vitro and in vivo—identification of reaction intermediates and oxidant-specific minor products. *Free Radic Biol Med* 99: 32–42, 2016.

Address correspondence to:
Dr. Alexander Ryan Lippert
Department of Chemistry
Southern Methodist University
Dallas, TX 75205
USA

E-mail: alippert@smu.edu

Date of first submission to ARS Central, August 23, 2021; date of acceptance, August 25, 2021.

Abbreviations Used

3-MST = 3-mercaptopyruvate sulfur transferase
CBS = cystathionine β-synthase
cGMP = cyclic guanosine monophosphate
CIEEL = chemically initiated electron exchange luminescence
CSE = cystathionine γ-lyase
Cys-SSH = cysteine persulfide
H_2O_2 = hydrogen peroxide
H_2S = hydrogen sulfide
H_2S_n = polysulfides
HNO = nitroxyl
$HO^{\bullet}$ = hydroxyl radical
HOCl = hypochlorite
HPLC = high-performance liquid chromatography
$HSO^{\bullet}$ = hydrosulfinyl radical
iNOS, NOS-2 = inducible nitric oxide synthase
L-012 = 8-amino-5-chloro-2,3-dihydro-7-phenyl-pyrido[3,4-d]pyridazine-1,4-dione
L-NAME = (ω)-nitro-L-arginine methyl ester
LPS = lipopolysaccharide
NIR = near-infrared
$NO^{\bullet}$ = nitric oxide
$NO_2^{\bullet}$ = nitrogen dioxide radical
NOS = nitric oxide synthase
O_2 = oxygen
O_3 = ozone
$ONOO^-$ = peroxynitrite
PeT = photoinduced electron transfer
SIN-1 = 3-morpholinosydnonimine
SO = sulfur monoxide
SO_2 = sulfur dioxide
SOD = superoxide dismutase